

advances.sciencemag.org/cgi/content/full/6/36/eabc1968/DC1

Supplementary Materials for

Ancient Beringian paleodiets revealed through multiproxy stable isotope analyses

Carrin M. Halfman*, Ben A. Potter*, Holly J. McKinney, Takumi Tsutaya, Bruce P. Finney, Brian M. Kemp,
Eric J. Bartelink, Matthew J. Wooller, Michael Buckley, Casey T. Clark, Jessica J. Johnson,
Brittany L. Bingham, François B. Lanoë, Robert A. Sattler, Joshua D. Reuther

*Corresponding author. Email: cmhalfman@alaska.edu (C.M.H.); rhovanion25@gmail.com (B.A.P.)

Published 4 September 2020, *Sci. Adv.* **6**, eabc1968 (2020)
DOI: 10.1126/sciadv.abc1968

The PDF file includes:

Supplementary Text
Tables S1 to S17
Figs. S1 to S6
References

Other Supplementary Material for this manuscript includes the following:

(available at advances.sciencemag.org/cgi/content/full/6/36/eabc1968/DC1)

Data file S1

Extended Description of Faunal Samples

Primary fauna (found in USR C3 and/or ubiquitous in the regional archaeofaunal record) (Tables S13 and S14) includes the following taxa:

- 1) Bison (*Bison priscus*). Very large mammal remains are present in USR C3, and bison is the most ubiquitous taxon in the regional zooarchaeological record for the terminal Pleistocene/early Holocene.
- 2) Salmon (*Oncorhynchus sp.*). Salmon is the most abundant taxon (relative NISP) in USR C3. All salmon specimens analyzed here were genetically identified as chum salmon (*O. keta*) (Tables S1 and S4). Because of the scarcity of unburned and well-preserved contemporaneous salmon remains, our sample includes a mix of terminal Pleistocene/early Holocene and later archaeological specimens.
- 3) Small game. This source is a combination of hare (*Lepus americanus*), ground squirrel (*Urocitellus parryii*), and grouse/ptarmigan (Tetraoninae). All taxa are present in USR C3 and are common in the regional zooarchaeological record for the terminal Pleistocene/early Holocene. Carbon and nitrogen stable isotope values are similar among the three taxa (Table S2), so they were combined *a priori* for mixing model analyses.
- 4) Wapiti (elk) (*Cervus canadensis*). Very large mammal remains are present in USR C3 and wapiti is the second most ubiquitous taxon in the regional zooarchaeological record for the terminal Pleistocene/early Holocene.
- 5) Whitefish (Coregoninae). Whitefish are present in USR C3 but cannot be identified to species. The $\delta^{13}\text{C}$ values of the whitefish specimens used in this study identify them as distinctly freshwater forms based on a comparison with data compiled in Halfman et al. (34).

Secondary fauna (not confirmed at USR C3 but occasionally present in the regional archaeofaunal record) (Tables S13-S14) includes the following taxa:

- 1) Caribou (*Rangifer tarandus*). Caribou are present in around 20% of the regional zooarchaeological assemblages for the terminal Pleistocene/early Holocene and when present are typically not abundant. Because of the rarity of this taxon for this time period, most specimens analyzed here are from late Holocene assemblages.

- 2) Sheep (*Ovis dalli*). Sheep are present in around 20% of the regional zooarchaeological assemblages for the terminal Pleistocene/early Holocene and when present are typically not abundant. Because of the rarity of this taxon for this time period, most specimens analyzed here are from late Holocene assemblages.
- 3) Waterfowl. Waterfowl (including ducks, geese, cranes, and swans) are absent in USR C3, which is unlikely due to preservation bias since small ptarmigan/grouse bones are well preserved. Because migratory waterfowl have different feeding areas throughout the year, the isotopic composition of their bone collagen, which turns over slowly, is not a good proxy for the isotopic composition of the tissues actually consumed by humans, such as muscle, which turns over rapidly and reflects the isotopic signatures of local feeding areas (75, 76). Therefore, we include published data from Choy et al. (31) on the isotopic composition of modern waterfowl muscle, and adjust the $\delta^{13}\text{C}$ values to account for the Suess effect (following the original publication) and for the offset between muscle and collagen for birds on controlled monotonous diets (75).

Excluded Taxa.

We excluded the following taxa that are rarely recorded in the regional zooarchaeological record in the terminal Pleistocene/early Holocene (Tables S13-S14) or that were unlikely to have been regularly consumed:

- 1) Carnivores (e.g., wolves, foxes, bears, otters, felids). Carnivores are absent in USR C3 except for wolf. While carnivores are present in low frequencies in the regional zooarchaeological record for the terminal Pleistocene/early Holocene, they are unlikely to have been regularly consumed (77).
- 2) Moose. Moose are rare in the regional zooarchaeological record for the terminal Pleistocene/early Holocene, and moose hunting is relatively new in the boreal forest (78).
- 3) Microtines. Microtines are present in USR C3 but are possibly intrusive and are unlikely to have been regularly consumed (79).
- 4) Other megafauna. Mammoth and horse were extinct in the region by ca. 14,000–13,000 cal BP (54).

- 5) Plants. Although plants were almost certainly collected and consumed (80), their nutrient composition is mostly carbohydrate, so they are unlikely to have contributed significantly to dietary protein.

In order to better capture intraspecific variation in $\delta^{13}\text{C}$ and $\delta^{15}\text{N}$ values, we have included specimens from later time periods for a limited number of taxa that are rare in the terminal Pleistocene/early Holocene archaeofaunal record, as indicated in the faunal descriptions. We recognize that there may be some temporal variation in isotope values among specimens from the same region. However, while fairly large isotopic shifts during the Holocene have been documented for several large herbivores in Northwest Europe (81, 82), this pattern does not seem apparent in eastern Beringia. For example, long-term records for caribou and moose bone collagen $\delta^{13}\text{C}$ and $\delta^{15}\text{N}$ values show little variation (<2.0‰) from around 15,000 BP to the last millennium on the North Slope of Alaska, with no clear temporal trends (83). For Pacific salmon, there are few long-term records. Isotopic data for modern sockeye salmon scales over a 100-year period generally show changes of only 1-1.5 ‰ or less for $\delta^{13}\text{C}$ and $\delta^{15}\text{N}$ values (84), while bone collagen from prehistoric salmon on Sanak Island, Alaska show non-significant differences in $\delta^{13}\text{C}$ and $\delta^{15}\text{N}$ values for most time periods over 4,500 years (60). In general, archaeological salmon bone collagen $\delta^{13}\text{C}$ and $\delta^{15}\text{N}$ values are similar throughout the North Pacific from various time periods, with typical mean $\delta^{13}\text{C}$ values of around -16.0‰ to -15.0‰ and typical mean $\delta^{15}\text{N}$ values of around 10.5‰ to 12.0‰ (34, 58, 60-62, 85). The mean $\delta^{13}\text{C}$ and $\delta^{15}\text{N}$ values for our salmon sample fall within these bounds, providing confidence that they are reasonable values to use in our mixing models.

Estimation of Season of Death for the USR Infants

Given high resolution archaeology at USR, we can estimate the season of death of the USR1 and USR2 individuals, and thereby estimate the temporal window of tissue formation and seasonal window of resource consumption. The infants were buried in a pit excavated within a central cooking hearth of a residential structure and backfilled with sediment containing burned fauna from earlier consumption events. After the interment, continued occupation of the feature and cooking episodes are represented by hearth fauna. Finally, a 3-year old child died (USR3) and was cremated within the hearth and the feature was abandoned. Faunal diversity is nearly identical between the pit fill and the hearth, with salmon and ground squirrel predominant (5),

suggesting the same (or similar) seasons of occupation. The most parsimonious scenario is use of the feature (and burials) within one season – with several faunal and floral taxa that provide more precise windows to estimate season of death of the infants. The integrity of the burial feature and articulation of the infants suggests that they were buried at the same time. Table S5 lists seasonally sensitive taxa for USR Component 3, derived from analyses in Potter et al. (5, 86), Halffman et al. (34), and Holloway (87).

Arctic ground squirrel (*Urocitellus parryii*) remains from both the cremation hearth (post-dating the infant burial) and the burial fill (predating the infant burial) contain immature individuals, based on unfused and partially fused long bones (humeri, femora, tibiae, radii). Both assemblages contain burned and processed fauna and are unlikely to be intrusive (5), and we expect from ethnographic data that small game was likely captured by snares (i.e., while active rather than while hibernating) (80). Modern arctic ground squirrel juveniles (young-of-the-year) emerge above ground in late June/early July (88). The availability of arctic ground squirrels begins to decline as early as late July when adult females begin entering hibernation, followed by juvenile females in mid-September and juvenile and adult males in late September/early October (88-90). The USR ground squirrel data suggest occupation sometime between July to September.

Anadromous chum salmon (*Oncorhynchus keta*) remains were identified through genetic and isotopic analyses (34) and are present in both burial fill and hearth matrices. Presently, two runs of chum salmon have been identified in the Tanana River: the summer run begins in early July and ends in mid- to late August, while the fall run begins in mid-August, peaks in mid-September, and continues into late fall, when freeze-up limits fishing on the river (28). Given the uncertainties involved in extrapolating to the Pleistocene/Holocene transition, it is difficult to *a priori* select between the two runs, or if they existed.

Several macrobotanical remains were identified in the hearth feature, but none were recovered from the burial fill (87). Seasonally available floral taxa within the hearth include *Arctostaphylos uva-ursi* (bearberry), *Rubus* cf. *R. arcticus* (nagoonberry) and *Vaccinium* spp. (bog blueberry/low-bush cranberry). The ripening and harvesting period is typically earliest for nagoonberry (July) and blueberry (July and August), followed by bearberry and low-bush cranberry (August and September) (87, 91).

Collectively, the immature ground squirrels and chum salmon in the burial fill and later hearth suggest an occupation between July and September. Multiple berry species have

overlapping ripening and harvesting periods between July and September. All seasonal indicators present in the hearth feature (postdating infant burial) potentially overlap around early August (Table S5).

A number of lines of evidence suggest the USR occupation occurred within a single season. There is no indication of multiple seasons of use, or of multi-year use. Both hearth and burial fill assemblages have a nearly identical suite of fauna from the same season. There is no evidence of feature blurring or palimpsests of lithics, fauna, or features. Lithic debris is not present in large quantities or densities, and there is limited evidence of sweeping or other camp cleaning activities suggesting long-term occupation. All of the lithic remains appear to be in primary deposition.

The most parsimonious scenario is that the two infants died between late July and early August, followed by interment with backfill incorporating earlier processing and/or consumption debris. The hearth saw continued use after the infant burials for a period of time where 827 NISP of fauna were preserved, including 326 salmon, 191 ground squirrel, and 46 hare specimens. These, along with the macrobotanical remains indicate the same season of occupation, or slightly later, between early to late August. Given a season of death between late July and early August, we can estimate the period of tissue formation (rib and tooth development), and thus the specific periods of the mothers' diets reflected in the infant samples.

Models of Fetal Bone Turnover Rates

We present here the first model of fetal bone turnover rates, where turnover consists of two components: modeling (bone growth) and remodeling (bone resorption/replacement or "turnover" in a narrow sense). In this model, bone modeling was estimated using published data on increases in fetal bone mass, and bone remodeling was estimated from age change in a bone resorption marker. Weekly changes in turnover rate of fetal bone collagen and mineral were computed by summing the effect of modeling and remodeling. The general strategy is similar with that used in Tsutaya and Yoneda, 2013 (15).

1. Datasets

a) Change in total skeletal mass in the fetal period

A function that describes changes in total skeletal mass in the fetal period was taken from equation (3) that appears on page 4 of Trotter and Hixon, 1974 (92). Original data range from 16 to 44 gestational weeks.

$$\text{Mass}[t] = 10^{0.0528 \times t - 0.0838} \quad (1)$$

b) Change in %ash of total skeleton in the fetal period

A function that describes changes in %ash of the total skeleton in the fetal period was calculated from extracted data from Figure 3 of Trotter and Hixon, 1974 (92). The extraction was done by one of us (CMH) using WebPlotDigitizer (93). Original data ranged from 16 to 44 gestational weeks.

$$P.\text{Ash}[t] = 0.0011960 \times t + 0.6159231 \quad (2)$$

c) Change in ICTP level in fetal period

A function that describes changes in ICTP (carboxyterminal telopeptide of type I collagen) level in umbilical cord blood by gestational age was taken from Figure 2-1 of Nakano et al., 2006 (94). Original data range from 27 to 42 gestational weeks.

$$\text{ICTP}[t] = -7.744 \times t + 386.256 \quad (3)$$

d) Remodeling rate of bone collagen at the time of birth

A value of $3.725 (\text{year}^{-1})$ was taken from Leggett et al., 1982 (95) for bone collagen remodeling rate at the age of 0 years. This value was estimated from fallout ^{90}Sr concentrations in skeletons from different ages.

2. Computation

a) Modeling

Weekly increase of skeletal mass (Eq. 1) was used as a proxy of modeling rate. To approximate the collagen and mineral portions of bone, skeletal mass was multiplied by $(1 - P.\text{Ash})$ and $P.\text{Ash}$, respectively (see Eq. 2). The collagen and mineral mass at gestational age of t weeks was expressed as:

$$\text{Col.Mass}[t] = \text{Mass}[t] \times (1 - P.\text{Ash}[t]) \quad (4)$$

$$\text{Min.Mass}[t] = \text{Mass}[t] \times \text{P.Ash}[t] \quad (5)$$

Modeling rates of collagen and mineral portions from gestational weeks $t-1$ to t were expressed as:

$$\text{Col.Mod}[t] = (\text{Col.Mass}[t] - \text{Col.Mass}[t-1]) / \text{Col.Mass}[t] \quad (6)$$

$$\text{Min.Mod}[t] = (\text{Min.Mass}[t] - \text{Min.Mass}[t-1]) / \text{Min.Mass}[t] \quad (7)$$

Because the age range of the original dataset is 16–44 gestational weeks, Eq. 4–7 are valid only in the same gestational age range.

b) Remodeling of collagen

Change in ICTP (biomarker for bone resorption) level (Eq. 3) was used as a proxy of the remodeling rate. In order to convert the ICTP level into a remodeling rate, resorption rate at the time of birth (3.725 year^{-1}) (95) was used for an anchor point. Remodeling rate of collagen from gestational age of $t-1$ to t weeks is expressed as:

$$\text{Col.Remod}[t] = \text{ICTP}[t] / \text{ICTP[BIRTH]} \times 3.725 \times 7 / 365 \quad (8)$$

In Eq. 8, correspondence between the ICTP level and the remodeling rate was assumed as linear and 1:1. BIRTH means gestational week at the time of birth. Furthermore, the unit of annual remodeling rate was simply divided with the number of weeks in a year to obtain the unit of weekly remodeling rate. Because the age range of the original dataset is 27–42 gestational weeks, Eq. 8 is valid only in the same gestational age range.

c) Remodeling of mineral

After the resorption of bone matrix, collagen matrix is formed first and then its mineralization occurs gradually. Therefore, the remodeling rate of bone mineral should be estimated from that of bone collagen by considering the delay of mineralization. Following Rauch and Schoenau, 2001 (96), 75% of the matrix is mineralized within first the few days and mineral continues to be incorporated during the following 6 months. To implement the recurrence function, mineralization low Lambda was simplified as the following:

$$\text{Lambda} = [0.7, 0.8, 0.9, 1.0] \quad (9)$$

This means that 70% of the matrix was mineralized within the first week, and the figure reaches 80%, 90%, and 100% at the end of second, third, and fourth weeks, respectively, after the formation of new collagen matrix. Difference of Lambda from the previous week was expressed as:

$$\text{Diff.Lambda} = [0.7, 0.1, 0.1, 0.1] \quad (10)$$

Considering the delay in mineralization, the remodeling rate of mineral from gestational age of $t-1$ to t weeks is expressed as:

$$\text{Min.Remod}[t] = \sum_{j=0}^3 (\text{Col. Remod}[t-j] \times \text{Diff. Lambda}[j+1] \times \text{Min.Mass}[t-j]) / \text{Min.Mass}[t] \quad (11)$$

In the modeling portion, there is no need to correct for the delay of mineralization because %ash was provided to the age change of skeletal mass (this procedure includes the concept of the delay in mineralization).

d) Turnover

Turnover (modeling + remodeling) rates of collagen and mineral from gestational age of $t-1$ to t weeks are expressed, respectively, as:

$$\text{Col.Tor}[t] = \text{Col.Remod}[t] \times \text{Col.Mass}[t-1] / \text{Col.Mass}[t] + (1 - \text{Col.Mass}[t-1]) / \text{Col.Mass}[t] \quad (12)$$

$$\text{Min.Tor}[t] = \text{Min.Remod}[t] \times \text{Min.Mass}[t-1] / \text{Min.Mass}[t] + (1 - \text{Min.Mass}[t-1]) / \text{Min.Mass}[t] \quad (13)$$

Because the conservative age range of original dataset is 27–42 gestational weeks for collagen and the recurrence function consumes the first 4 weeks for mineral, Eq. 12 and 13 are valid only in 27–42 and 31–42 gestational weeks, respectively.

e) Postnatal turnover

Turnover (modeling + remodeling) rates of collagen and mineral from postnatal age of $t-1$ to t weeks were calculated from the NLS (nonlinear least squares) functions of infant bone collagen and mineral turnover rates (15). Integrated turnover rates from 0 to 6 weeks after birth and from

2 to 6 weeks were used for postnatal turnover rate during the period of 0 to 6 weeks postnatal and 2 to 6 weeks postnatal. NLS functions are as follows [the NLS function for collagen was indicated in Tsutaya and Yoneda, 2013 (15), but that for mineral is newly calculated from values that are shown in Tsutaya and Yoneda, 2013 (15)]:

$$\text{Col.TorPN}[t] = 1.778 - 0.4121 \times t + 0.05029 \times t^2 - 0.002756 \times t^3 + 0.0005325 \times t^4 \quad (14)$$

$$\text{Min.TorPN}[t] = 1.433 - 0.2966 \times t + 0.03531 \times t^2 - 0.001938 \times t^3 + 0.00003749 \times t^4 \quad (15)$$

3. Simulation

a) Assumptions 1

- BIRTH = 40 gestational weeks (97).
- There is no time lag between the isotopic change in dietary input and elemental routing to bone. (i.e., there is no contribution of stored amino acid pool in the body).
- (1 – P.Ash) and P.Ash represent the mass of collagen and mineral portions of bone, respectively (Eq. 2).
- Correspondence between ICTP level and remodeling rate was assumed as linear and 1:1 (Eq. 8).
- The unit of annual remodeling rate was simply divided by the number of weeks in a year to obtain the unit of weekly remodeling rate (Eq. 8).

b) Results

Table S6 indicates the weekly turnover, remodeling, and modeling rates by gestational and postnatal ages (weeks). These values indicate the rates from $x-1$ to x gestational weeks. For example, numbers in the row for GA=33 represent the rates during the period from 32 to 33 gestational weeks (from just after the completion of the 32nd week/beginning of the 33rd week to the end of the 33rd week). For postnatal values, “0–6 PW” represents the turnover rate from 0 to 6 weeks after birth (from the beginning of the 1st week to the end of the 6th week), and “0–3 PW” represents the turnover rate from 0 to 3 weeks after birth (from the beginning of the 1st week to the end of the 3rd week) in the infant.

4. Proportion of weekly fraction at a given age

It can be assumed that bone tissue at a given age consists of a number of incorporated fractions during each previous week. These fractions have experienced remodeling at each week, and its proportion at a given age can be calculated from the product of the cumulative effect of

remodeling and its original mass at the point of incorporation. These parameters can be calculated as shown below. Results are shown in Table S7.

a) Initial mass of weekly fractions

Mass of a newly incorporated fraction of collagen or mineral from gestational age of $t-1$ to t weeks is calculated as:

$$\text{Col.New}[t] = \text{Col.Mass}[t] \times \text{Col.Tor}[t] \quad (16)$$

$$\text{Min.New}[t] = \text{Min.Mass}[t] \times \text{Min.Tor}[t] \quad (17)$$

b) Cumulative effect of remodeling

The cumulative effect of remodeling from gestational age t (minimum $t = 28$ for collagen and minimum $t = 32$ for mineral, see Table S7) to T is calculated as:

$$\text{Col.Remod.Cuml}[t, T] = \prod_{x=t}^T (1 - \text{Col.Remod}[x]) \quad (18)$$

$$\text{Min.Remod.Cuml}[t, T] = \prod_{x=t}^T (1 - \text{Col.Remod}[x]) \quad (19)$$

c) Proportion at given gestational ages

The fraction of the total that was incorporated into bone from gestational age of $t-1$ to t weeks, at gestational age T is calculated as:

$$\text{Col.Prop}[t, T] = \text{Col.New}[t] \times \text{Col.Remod.Cuml}[t, T] / \text{Col.Mass}[T] \quad (20)$$

when $t = 28$, $\text{Col.New}[t]$ should be $\text{Col.Mass}[28]$

$$\text{Min.Prop}[t, T] = \text{Min.New}[t] \times \text{Min.Remod.Cuml}[t, T] / \text{Min.Mass}[T] \quad (21)$$

when $t = 32$, $\text{Min.New}[t]$ should be $\text{Min.Mass}[32]$

The mass of the first fraction should include those of all fractions that were formed before, and thus $\text{Mass}[t]$ is used instead of $\text{New}[t]$ when $t = 28$ for collagen and $t = 32$ for mineral.

For example, the proportion at birth (40 gestational weeks) is calculated from fractions incorporated during 27–40 weeks for collagen and 31–40 weeks for mineral. Table S7 shows that for the bone collagen existing at 40 GW, 17.2% was formed in the 40th week (from just after the end of the 39th week/beginning of the 40th week to through the end of the 40th week), 14.7% was formed in the 39th week, 12.5% was formed in the 38th week, etc. Weekly fractions may be

summed to calculate the proportion of tissue formed over a combination of weeks; for example, for the bone collagen existing at 40 GW, a total of 55% was formed in the previous 4 weeks (36–40th week, from just after the end of the 36th week/beginning of the 37th week through the end of the 40th week). Alternatively, the turnover rate during the period of the last 4 weeks (36–40th week: from just after completion of the 36th week/beginning of the 37th week to the end of the 40th week) before birth (40th week) is calculated as:

$$1 - (1 - 0.174) \times (1 - 0.180) \times (1 - 0.186) \times (1 - 0.192) = 0.5545185$$

The proportion at 33 gestational weeks (the estimated age-at-death for USR2) is calculated from fractions incorporated during 27–33 weeks for collagen and 31–33 weeks for mineral. For example, Table S7 shows that for bone collagen existing at 33 GW, 21.5% was formed during the 33rd week (from just after the completion of the 32nd week through the 33rd week), 17.3% was formed in the 32nd week, and 13.9% was formed in the 31st week. A total of 63.7% of bone collagen was formed in the previous four weeks (29–33rd week: from just after completion of the 29th week/beginning of the 30th week through the end of the 33rd week).

d) Proportion at given postnatal ages

Since the process and dataset to calculate postnatal bone turnover rates differ from gestational ones, the proportion of postnatal fractions can only be calculated as a single aggregated one for several weeks. For example, integrated turnover rate (equations 14 and 15) from 0 to 3.0 weeks after birth is 0.1042 for collagen and 0.0840 for mineral. Therefore, it can be estimated that approximately 10.42% of collagen mass and 8.0% of mineral mass have been incorporated after birth and the proportions of gestational fractions have been decreased to 89.58% for collagen and 91.60% for mineral, at 3 postnatal weeks. The proportion for USR1 (if age-at-death was 3 postnatal weeks) can be calculated as such and is shown in Table S7.

Table S1. Human and faunal bone samples used for stable isotope analysis. Abbreviations: yr BP, radiocarbon years before present (present = 1950 AD); cal yr BP, calibrated years before present (present = 1950 AD); ZooMS, Zooarchaeology by Mass Spectrometry (46); UAF, University of Alaska Fairbanks; UAMN, University of Alaska Museum of the North; TCC, Tanana Chiefs Conference.

Taxon	Lab ID	Site & Component	Date (yr BP \pm 1 SD)	Date (cal yr BP, 2- σ)	Repository & ID	Element	DNA ID	ZooMS ID	Morphological ID
Human									
<i>Homo sapiens</i>	USR1	Upward Sun River C3	9990 \pm 30	11,610–11,280	UAF (USR1)	rib	<i>H. sapiens</i> ^a	--	<i>H. sapiens</i>
<i>Homo sapiens</i>	USR2	Upward Sun River C3	9990 \pm 30	11,610–11,280	UAF (USR2)	rib	<i>H. sapiens</i> ^a	--	<i>H. sapiens</i>
Primary fauna									
Bison									
<i>Bison priscus</i>	16.178	Gerstle C3	8880 \pm 20	10,160–9910	UAMN (UA2001-71-1121)	humerus	--	--	<i>B. priscus</i>
<i>Bison priscus</i>	16.179	Gerstle C3	8880 \pm 20	10,160–9910	UAMN (UA99-62-0950)	metatarsal	<i>B. priscus</i>	<i>Bison/Bos</i>	<i>B. priscus</i>
<i>Bison priscus</i>	16.180	Gerstle LLD	--	undated	UAMN (UA97-061-214)	calcaneus	<i>B. priscus</i>	<i>Bison/Bos</i>	<i>B. priscus</i>
<i>Bison priscus</i>	16.181	Gerstle LLD	9506 \pm 38	11,072–10,659	UAMN (UA97-061-231)	metatarsal	<i>B. priscus</i>	<i>Bison/Bos</i>	<i>B. priscus</i>
<i>Bison priscus</i>	16.182	Gerstle LLD	9400 \pm 60	11,040–10,430	UAMN (UA97-061-229)	metatarsal	<i>B. priscus</i>	<i>Bison/Bos</i>	<i>B. priscus</i>
<i>Bison priscus</i>	16.184	Gerstle C3	8880 \pm 20	10,160–9910	UAMN (UA2001-71-1297)	metacarpal	<i>B. priscus</i>	<i>Bison/Bos</i>	<i>B. priscus</i>
<i>Bison priscus</i>	16.185	Gerstle C3	8880 \pm 20	10,160–9910	UAMN (UA2001-71-1288)	innominate	--	<i>Bison/Bos</i>	<i>B. priscus</i>
<i>Bison priscus</i>	17.276	Delta River Overlook C3	8634 \pm 27	9662–9562	UAF (DRO-4-17)	mandible	<i>B. priscus</i>	--	<i>B. priscus</i>
<i>Bison priscus</i>	17.277	Delta River Overlook C3	8634 \pm 27	9662–9562	UAF (DRO-9-103)	long bone	--	<i>Bison/Bos</i>	VL Artiodactyla
<i>Bison priscus</i>	17.280	Delta River Overlook C4	7630 \pm 30	8512–8379	UAF (DRO-8-25)	rib	--	<i>Bison/Bos</i>	VL Artiodactyla
Salmon									
<i>Oncorhynchus keta</i>	15.301	Upward Sun River C3	9990 \pm 30	11,610–11,280	UAF(USR-58-30)	vertebra	<i>O. keta</i> ^b	--	<i>Oncorhynchus</i> . sp.
<i>Oncorhynchus keta</i>	16.109	XBD-318	10,830 \pm 40	12,680–12,770	UAMN (UA2006-106-0009)	vertebra	<i>O. keta</i>	--	<i>Oncorhynchus</i> . sp.
<i>Oncorhynchus keta</i>	17.106	Rampart Dune	650 \pm 20	666–560	TCC (Pit Q salmon)	articular	<i>O. keta</i>	--	<i>Oncorhynchus</i> . sp.
<i>Oncorhynchus keta</i>	17.109	Healy Lake Upper Cultural	--	historic	UAMN (69-49-4006)	quadrate	<i>O. keta</i>	--	<i>Oncorhynchus</i> . sp.
<i>Oncorhynchus keta</i>	17.110	Healy Lake Upper Cultural	--	historic	UAMN (69-49-4006)	opercle	<i>O. keta</i>	--	<i>Oncorhynchus</i> . sp.
<i>Oncorhynchus keta</i>	17.111	Healy Lake Upper Cultural	--	historic	UAMN (69-49-4006)	dentary	<i>O. keta</i>	--	<i>Oncorhynchus</i> . sp.

Taxon	Lab ID	Site & Component	Date (yr BP ± 1 SD)	Date (cal yr BP, 2-σ)	Repository & ID	Element	DNA ID	ZooMS ID	Morphological ID
<i>Oncorhynchus keta</i>	17.112	Healy Lake Upper Cultural	--	historic	UAMN (69-49-4006)	articular	<i>O. keta</i>	--	<i>Oncorhynchus</i> . sp.
Small game: ground squirrel									
<i>Urocitellus parryii</i>	16.158	Upward Sun River C3	9990 ± 30	11,610–11,280	UAF(USR-58-326)	femur	--	--	<i>U. parryii</i>
<i>Urocitellus parryii</i>	16.159	Mead C3	10,270 ± 20	12,120–11,850	UAF(MEA-60-189)	femur	--	--	<i>U. parryii</i>
<i>Urocitellus parryii</i>	16.161	Mead C3	10,270 ± 20	12,120–11,850	UAF(MEA-73-431)	femur	--	--	<i>U. parryii</i>
<i>Urocitellus parryii</i>	16.162	Mead C4	11,080 ± 20	13,110–12,790	UAF(MEA-71-832)	ulna	--	--	<i>U. parryii</i>
<i>Urocitellus parryii</i>	16.163	Mead C3	10,270 ± 20	12,120–11,850	UAF(MEA-78-323)	femur	--	--	<i>U. parryii</i>
<i>Urocitellus parryii</i>	16.164	Mead C4	11,080 ± 20	13,110–12,790	UAF(MEA-86-1079)	humerus	--	--	<i>U. parryii</i>
<i>Urocitellus parryii</i>	16.165	Mead C3	10,270 ± 20	12,120–11,850	UAF(MEA-80-374)	femur	--	--	<i>U. parryii</i>
Small game: grouse/ptarmigan									
Tetraoninae	16.188	Upward Sun River C1	11,320 ± 30	13,300–13,120	UAF(USR-78-2)	ulna	--	--	Tetraoninae
Tetraoninae	16.190	Upward Sun River C2	10,140 ± 40	11,990–11,510	UAF(USR-36-13)	humerus	--	--	Tetraoninae
Tetraoninae	16.191	Mead C3	10,270 ± 20	12,120–11,850	UAF(MEA-86-1015)	scapula	--	--	Tetraoninae
Tetraoninae	16.192	Mead C3	10,270 ± 20	12,120–11,850	UAF(MEA-72-450)	femur	--	--	Tetraoninae
Small game: hare									
<i>Lepus americanus</i>	16.151	Upward Sun River C3	9990 ± 30	11,610–11,280	UAF(USR-H-316a)	calcaneus	--	--	<i>L. americanus</i>
<i>Lepus americanus</i>	16.152	Mead C3	10,270 ± 20	12,120–11,850	UAF(MEA-72-341)	innominate	--	--	<i>L. americanus</i>
<i>Lepus americanus</i>	16.237	Mead C3	10,270 ± 20	12,120–11,850	UAF(MEA-72-228)	scapula	--	--	<i>L. americanus</i>
<i>Lepus americanus</i>	16.238	Mead C3	10,270 ± 20	12,120–11,850	UAF(MEA-78-472)	scapula	--	--	<i>L. americanus</i>
<i>Lepus americanus</i>	16.239	Mead C3	10,270 ± 20	12,120–11,850	UAF(MEA-86-808)	vertebra	--	--	<i>L. americanus</i>
Wapiti									
<i>Cervus canadensis</i>	16.168	Gerstle C3	8880 ± 20	10,160–9910	UAMN (UA2000-54-289)	metatarsal	--	Cervidae, consistent with <i>Cervus</i>	<i>C. canadensis</i>
<i>Cervus canadensis</i>	16.169	Gerstle C3	8880 ± 20	10,160–9910	UAMN (UA99-62-0803c)	sacrum	--	--	<i>C. canadensis</i>
<i>Cervus canadensis</i>	16.170	Gerstle C3	8880 ± 20	10,160–9910	UAMN (UA99-62-0801)	radius	--	Cervidae, consistent with <i>Cervus</i>	<i>C. canadensis</i>
<i>Cervus canadensis</i>	16.171	Gerstle LLD	--	undated	UAMN (UA00-54-0002)	metacarpal	<i>C. canadensis</i>	Cervidae, consistent with <i>Cervus</i>	<i>C. canadensis</i>
<i>Cervus canadensis</i>	16.173	Gerstle C3	8880 ± 20	10,160–9910	UAMN (UA99-62-0802)	ulna	--	Cervidae, consistent with <i>Cervus</i>	<i>C. canadensis</i>
<i>Cervus canadensis</i>	16.174	Gerstle C3	8880 ± 20	10,160–9910	UAMN (UA2001-71-452)	tibia	--	Cervidae, consistent with <i>Cervus</i>	<i>C. canadensis</i>
<i>Cervus canadensis</i>	16.175	Gerstle C3	8880 ± 20	10,160–9910	UAMN (UA2003-54-1518)	tibia	<i>C. canadensis</i>	Cervidae, consistent with <i>Cervus</i>	<i>C. canadensis</i>

Taxon	Lab ID	Site & Component	Date (yr BP ± 1 SD)	Date (cal yr BP, 2-σ)	Repository & ID	Element	DNA ID	ZooMS ID	Morphological ID
<i>Cervus canadensis</i>	16.177	Gerstle LLD	--	undated	UAMN (UA00-054-0005)	femur	--	Cervidae, consistent with <i>Cervus</i>	<i>C. canadensis</i>
<i>Cervus canadensis</i>	16.186	Gerstle LLD	--	undated	UAMN (UA99-62-800e)	vertebra	--	Cervidae, consistent with <i>Cervus</i>	<i>C. canadensis</i> or <i>B. priscus</i>
<i>Cervus canadensis</i>	16.205	Hollembaek	7020 ± 30	7934–7792	UAMN (UA2016-062-0751)	calcaneus	--	Cervidae, consistent with <i>Cervus</i>	<i>C. canadensis</i>
<i>Cervus canadensis</i>	17.260	Gottschling	9040 ± 30	10,241–10,186	UAMN (UA2016-129-0067)	metatarsal	--	Cervidae, consistent with <i>Cervus</i>	<i>C. canadensis</i>
<i>Cervus canadensis</i>	17.271	Delta River Overlook C2a	10,000 ± 40	11,700–11,274	UAF(DRO-1-54)	long bone	--	Cervidae, consistent with <i>Cervus</i>	VL Artiodactyla
<i>Cervus canadensis</i>	17.272	Delta River Overlook C2a	10,000 ± 40	11,700–11,274	UAF(DRO-4-291)	long bone	--	Cervidae, consistent with <i>Cervus</i>	VL Artiodactyla
<i>Cervus canadensis</i>	17.279	Delta River Overlook C4	7630 ± 30	8512–8379	UAF(DRO-2-42)	long bone	--	Cervidae, consistent with <i>Cervus</i>	VL Artiodactyla
<i>Cervus canadensis</i>	17.281	Delta River Overlook C5	6680 ± 175	7924–7255	UAF(DRO-2-33)	ulna	--	Cervidae, consistent with <i>Cervus</i>	<i>C. canadensis</i>
<i>Cervus canadensis</i>	17.282	Delta River Overlook C5	6680 ± 175	7924–7255	UAF(DRO-2-35)	long bone	--	Cervidae, consistent with <i>Cervus</i>	VL Artiodactyla
Whitefish									
Coregoninae	17.101	Hollembaek	9320 ± 30	10,423–10,647	UAMN (UA2016-062-0318)	vertebra	--	--	Coregoninae
Coregoninae	17.102	Hollembaek	9320 ± 30	10,423–10,647	UAMN (UA2016-062-0359)	vertebra	--	--	Coregoninae
Coregoninae	17.103	Hollembaek	9320 ± 30	10,423–10,647	UAMN (UA2016-062-0359)	vertebra	--	--	Coregoninae
Coregoninae	17.104	Hollembaek	9320 ± 30	10,423–10,647	UAMN (UA2016-062-0360)	vertebra	--	--	Coregoninae
Coregoninae	17.105	Hollembaek	9320 ± 30	10,423–10,647	UAMN (UA2016-062-0360)	vertebra	--	--	Coregoninae
Secondary fauna									
Caribou									
<i>Rangifer tarandus</i>	16.113	Carlo Creek	9866 ± 55	11,217–11,314	UAMN (UA76-212-0123)	phalanx	--	<i>Rangifer</i>	<i>R. tarandus</i>
<i>Rangifer tarandus</i>	16.114	Carlo Creek	9866 ± 55	11,217–11,314	UAMN (UA76-212-0330)	metacarpal	--	<i>Rangifer</i>	<i>R. tarandus</i>
<i>Rangifer tarandus</i>	16.115	Dixthada A	622 ± 31	659–551	UAMN	metatarsal	--	<i>Rangifer</i>	<i>R. tarandus</i>

TAXON	LAB ID	SITE & COMPONENT	DATE (YR BP ± 1 SD)	DATE (CAL YR BP, 2-σ)	REPOSITORY & ID	ELEMENT	DNA ID	ZOOAMS ID	MORPHOLOGICAL ID
<i>Rangifer tarandus</i>	16.116	Dixthada A	622 ± 31	659–551	UAMN (UA69-0881)	phalanx	--	<i>Rangifer</i>	<i>R. tarandus</i>
<i>Rangifer tarandus</i>	16.117	Nenana River Gorge	320 ± 63	505–154	UAMN (60N/14W)	radius	--	<i>Rangifer</i>	<i>R. tarandus</i>
<i>Rangifer tarandus</i>	16.118	Nenana River Gorge	320 ± 63	505–154	UAMN (59N/14W)	metatarsal	--	<i>Rangifer</i>	<i>R. tarandus</i>
<i>Rangifer tarandus</i>	16.119	Nenana River Gorge	320 ± 63	505–154	UAMN (58N/13W)	metatarsal	--	<i>Rangifer</i>	<i>R. tarandus</i>
<i>Rangifer tarandus</i>	16.120	Nenana River Gorge	320 ± 63	505–154	UAMN (58N/15W)	tarsal	--	<i>Rangifer</i>	<i>R. tarandus</i>
<i>Rangifer tarandus</i>	16.121	Nenana River Gorge	320 ± 63	505–154	UAMN (57N/14W)	metacarpal	--	<i>Rangifer</i>	<i>R. tarandus</i>
<i>Rangifer tarandus</i>	16.122	Nenana River Gorge	320 ± 63	505–154	UAMN (55N/10W)	metacarpal	--	<i>Rangifer</i>	<i>R. tarandus</i>
<i>Rangifer tarandus</i>	17.284	Delta River Overlook C6	5980 ± 30	6894–6737	UAF(DRO-5-4.1)	radius	<i>R. tarandus</i>	--	<i>R. tarandus</i>
Sheep									
<i>Ovis dalli</i>	16.134	Carlo Creek	9866 ± 55	11,217–11,314	UAMN (UA75-011-0007)	phalanx	--	Ovine	<i>O. dalli</i>
<i>Ovis dalli</i>	16.135	Nenana River Gorge	622 ± 31	659–551	UAMN (UA75-45-252)	astragalus	--	Ovine	<i>O. dalli</i>
<i>Ovis dalli</i>	16.136	Nenana River Gorge	622 ± 31	659–551	UAMN (UA75-45-244)	ulna	--	Ovine	<i>O. dalli</i>
<i>Ovis dalli</i>	16.137	Nenana River Gorge	622 ± 31	659–551	UAMN (58N/14W)	tibia	--	Ovine	<i>O. dalli</i>
<i>Ovis dalli</i>	16.139	Nenana River Gorge	622 ± 31	659–551	UAMN (UA75-45-250)	metapodial	--	Ovine	<i>O. dalli</i>
<i>Ovis dalli</i>	16.140	Nenana River Gorge	622 ± 31	659–551	UAMN (UA75-45-246)	patella	--	Ovine	<i>O. dalli</i>

Notes. Site dating references and additional information: (1) Carlo Creek (HEA-031) (98); (2) Delta River Overlook (XMH-297) (99); (3) Dixthada (TNX-004) (100); (4) Dock Site (XBD-361) (101); (5) Gerstle Component 3 (XMH-246) (30). (6) Gerstle LLD (Lower Locus, Disturbed) (XMH-246): Two bison specimens (16.181 and 16.182) were directly dated to 9506 ± 38 and 9400 ± 55 (OxA-11246 and Oxa-11962, respectively) (102, 103). The remaining LLD specimens have not been directly dated. The specimens may date to the period of site occupation (ca. 11,250–8,000 cal yr BP) or somewhat older given a date of 18,710–17,580 cal yr BP on an *Equus* specimen from the disturbed area (102). The limiting dates for wapiti presence in Alaska are ca. 15,200–5100 cal yr BP (104); (7) Gottschling (XBD-444). The wapiti specimen (17.260) was directly dated to 9040 ± 30 yr BP (UGAMS 30063) (this study); (8) Healy Lake Village (XBD-020): The Upper Cultural layer of the Healy Lake Village site is a historic Upper Tanana Athabaskan component dating to approximately the late 19th to early 20th centuries (105). We assume that for the salmon specimens from this component, the Suess effect on the $\delta^{13}\text{C}$ values is negligible (106), which is supported by the similarities in $\delta^{13}\text{C}$ values between the Healy Lake Village specimens and the prehistoric specimens; (9) Hollembaek (XBD-376). Whitefish specimen 17.102 was directly dated to 9320 ± 30 yr BP (UGAMS 32232) (this study); no freshwater reservoir correction has been applied to this date. Additional whitefish specimens from the same component are assumed to date to the same time period. The wapiti specimen (16.205) was directly dated to 7020 ± 30 yr BP (UGAMS 26195) (this study); (10) Mead (30); (11) Nenana River Gorge (100); (12) Rampart Dune, Pit Q. Birch bark associated with salmon specimen 17.106 was dated to 650 ± 20 yr BP (UGAMS

43632) (this study); **(13)** Shoreline Site (XBD-159) (101); **(14)** Upward Sun River (30); **(15)** XBD-318: Salmon specimen 16.109 was directly dated to $10,830 \pm 40$ BP (UGAMS 26403) (this study); this date does not include a marine reservoir correction. See also (35).

ZooMS identifications: *Bison/Bos* specimens are presumed to be *Bison*, given the absence of *Bos* dated to the early Holocene in the region. Specimens designated “Cervidae consistent with *Cervus*” are presumed to be wapiti (*Cervus canadensis*) because: (a) they exhibit collagen peptide markers that are consistent with *Cervus* and are inconsistent with *Rangifer* (46); (b) while no collagen peptide markers have been published to discriminate *Alces* from *Cervus*, the former taxon is rare in terminal Pleistocene/early Holocene zooarchaeological assemblages in the region (30); and (c) the only Cervidae taxa dated to this time period in the region are *Cervus*, *Rangifer*, and *Alces* (54, 107).

^aDNA results from previous studies (6, 7).

^bDNA results from previous study (34).

Table S2. Bone collagen $\delta^{13}\text{C}$ and $\delta^{15}\text{N}$ values for the USR infants and potential food sources. See Table S1 for sample descriptions.

Taxon	Study ID	Isotope Lab ID	$\delta^{13}\text{C} (\text{\textperthousand})$	$\delta^{15}\text{N} (\text{\textperthousand})$	%C	%N	C:N	%Yield
Human								
<i>H. sapiens</i>	USR1 ^a	G-116714	-18.4	9.1	43.4	15.7	3.2	9.1
<i>H. sapiens</i>	USR2	G-118722	-18.4	8.7	44.3	15.7	3.3	8.3
Primary fauna								
Bison								
<i>B. priscus</i>	16.178	G-166796	-21.5	3.5	40.8	13.6	3.5	3.4
<i>B. priscus</i>	16.179	G-158405	-21.7	2.4	50.0	17.7	3.3	6.9
<i>B. priscus</i>	16.180	G-158482	-21.4	5.8	45.4	16.5	3.2	11.1
<i>B. priscus</i>	16.181	G-158406	-22.5	2.6	42.3	14.0	3.5	12.6
<i>B. priscus</i>	16.182	G-158483	-21.4	5.5	45.4	16.2	3.3	7.9
<i>B. priscus</i>	16.184	G-158484	-21.4	6.2	44.8	15.5	3.4	7.0
<i>B. priscus</i>	16.185	G-166797	-21.8	5.7	41.2	13.7	3.5	4.4
<i>B. priscus</i>	17.276	G-171741	-21.1	5.2	42.8	14.8	3.4	5.1
<i>B. priscus</i>	17.277	G-171742	-20.9	5.0	37.2	12.5	3.5	3.0
<i>B. priscus</i>	17.280	G171745	-21.7	5.2	43.6	15.1	3.4	8.5
n			10	10				
Mean			-21.5	4.7				
SD			0.4	1.4				
Salmon								
<i>O. keta</i>	15.301 ^b	G-118723	-15.1	12.6	43.1	15.8	3.2	6.9
<i>O. keta</i>	16.109	G-147956	-16.3	11.2	40.0	14.6	3.2	8.9
<i>O. keta</i>	17.106	G-166798	-15.9	12.7	43.2	15.9	3.2	12.2
<i>O. keta</i>	17.109	G-166908	-16.1	9.9	40.9	15.5	3.1	12.6
<i>O. keta</i>	17.110	G-166909	-16.4	10.5	39.6	14.9	3.1	4.5
<i>O. keta</i>	17.111	G-166910	-16.0	11.4	38.6	14.4	3.1	5.5
<i>O. keta</i>	17.112	G-166911	-15.8	11.1	40.0	15.1	3.1	4.6
n			7	7				
Mean			-15.9	11.3				
SD			0.4	1.0				
Small Game								
<i>U. parryii</i>	16.158	G-147962	-20.8	1.8	40.3	13.4	3.5	1.1
<i>U. parryii</i>	16.159	G-162878	-22.8	1.1	39.2	13.3	3.5	2.2
<i>U. parryii</i>	16.161	G-162879	-22.6	1.6	43.7	15.6	3.3	6.0
<i>U. parryii</i>	16.162	G-158473	-22.0	0.5	44.7	15.6	3.3	5.3
<i>U. parryii</i>	16.163	G-158397	-21.1	2.0	43.9	15.6	3.3	12.6
<i>U. parryii</i>	16.164	G-158474	-21.5	1.5	42.8	14.1	3.5	1.7
<i>U. parryii</i>	16.165	G-158398	-19.6	1.3	41.6	14.6	3.3	5.1
Tetraoninae	16.188	G-158486	-21.1	0.6	43.7	14.5	3.5	2.8
Tetraoninae	16.190	G-158487	-20.6	1.2	44.4	15.7	3.3	5.4
Tetraoninae	16.191	G-158411	-21.0	0.3	40.1	13.5	3.5	1.9
Tetraoninae	16.192	G-158488	-20.7	1.2	44.8	15.8	3.3	6.7
<i>L. americanus</i>	16.151	G-167352	-22.3	2.6	39.5	13.3	3.5	2.2
<i>L. americanus</i>	16.152	G-158470	-21.9	0.0	40.6	13.7	3.5	3.8
<i>L. americanus</i>	16.237	G-158430	-21.9	0.1	43.7	15.5	3.3	6.4
<i>L. americanus</i>	16.238	G-158506	-22.3	1.2	41.6	13.8	3.5	2.7
<i>L. americanus</i>	16.239	G-158431	-22.2	1.3	41.5	13.8	3.5	3.4
n			16	16				
Mean			-21.5	1.1				
SD			0.9	0.7				
Wapiti								
<i>C. canadensis</i>	16.168	G-158476	-21.0	1.5	43.6	14.7	3.5	3.2
<i>C. canadensis</i>	16.169	G-158400	-20.1	1.5	42.4	15.3	3.2	2.9

TAXON	STUDY ID	ISOTOPE LAB ID	$\delta^{13}\text{C}$ (‰)	$\delta^{15}\text{N}$ (‰)	%C	%N	C:N	%Yield
<i>C. canadensis</i>	16.170	G-158477	-20.9	2.2	42.4	14.2	3.5	2.4
<i>C. canadensis</i>	16.171	G-158401	-20.9	1.9	38.5	12.7	3.5	7.5
<i>C. canadensis</i>	16.173	G-158402	-21.2	1.5	39.0	14.2	3.2	3.7
<i>C. canadensis</i>	16.174	G-166793	-21.8	2.7	29.1	9.9	3.4	1.7
<i>C. canadensis</i>	16.175	G-166794	-21.6	3.6	44.1	15.8	3.3	3.8
<i>C. canadensis</i>	16.177	G-158404	-21.2	1.3	42.2	15.3	3.2	5.6
<i>C. canadensis</i>	16.186	G-158485	-20.5	1.2	42.7	14.4	3.4	2.4
<i>C. canadensis</i>	16.205	G-171735	-21.1	3.8	38.8	13.6	3.3	3.7
<i>C. canadensis</i>	17.260	UGAMS 30063	-20.8	2.6	42.3	15.0	3.3	11.9
<i>C. canadensis</i>	17.271	G-171736	-19.8	3.2	42.4	14.9	3.3	10.5
<i>C. canadensis</i>	17.272	G-171737	-19.9	2.4	40.8	13.7	3.5	4.4
<i>C. canadensis</i>	17.279	G-171744	-20.7	0.8	42.8	14.6	3.4	5.9
<i>C. canadensis</i>	17.281	G-171746	-20.1	1.4	42.1	14.5	3.4	4.5
<i>C. canadensis</i>	17.282	G-171747	-19.9	1.4	43.2	15.2	3.3	7.7
n			16	16				
Mean			-20.7	2.1				
SD			0.6	0.9				
Whitefish								
Coregoninae	17.101	G-166901	-23.1	8.4	39.8	14.2	3.3	13.6
Coregoninae	17.102	G-166902	-25.1	10.2	41.7	15.6	3.1	13.1
Coregoninae	17.103	G-166903	-24.8	10.2	41.8	15.5	3.1	10.6
Coregoninae	17.104	G-166904	-24.7	10.3	42.1	15.6	3.2	12.2
Coregoninae	17.105	G-166905	-25.4	10.2	42.1	15.7	3.1	14.5
n			5	5				
Mean			-24.6	9.9				
SD			0.9	0.8				
Secondary fauna								
Caribou								
<i>R. tarandus</i>	16.113	G-158376	-18.2	1.0	43.7	15.1	3.4	4.5
<i>R. tarandus</i>	16.114	G-158452	-18.4	0.9	42.9	14.8	3.4	3.5
<i>R. tarandus</i>	16.115	G-158377	-18.0	3.3	45.3	16.0	3.3	7.7
<i>R. tarandus</i>	16.116	G-167351	-19.8	5.3	44.3	16.0	3.2	12.6
<i>R. tarandus</i>	16.117	G-158378	-18.5	2.4	43.5	14.4	3.5	4.2
<i>R. tarandus</i>	16.118	G-158454	-18.4	2.9	44.3	15.0	3.4	6.5
<i>R. tarandus</i>	16.119	G-158379	-18.1	2.0	44.4	15.4	3.4	6.3
<i>R. tarandus</i>	16.120	G-158455	-18.9	2.8	43.5	14.4	3.5	5.2
<i>R. tarandus</i>	16.121	G-158380	-18.7	2.4	44.7	15.2	3.4	6.7
<i>R. tarandus</i>	16.122	G-158456	-18.5	2.4	44.9	15.8	3.3	6.6
<i>R. tarandus</i>	17.284	G-171748	-17.4	2.0	44.6	15.8	3.3	16.7
n			11	11				
Mean			-18.4	2.5				
SD			0.6	1.2				
Sheep								
<i>O. dalli</i>	16.134	G-158462	-19.8	1.2	42.2	14.5	3.4	9.1
<i>O. dalli</i>	16.135	G-158387	-21.6	2.6	27.7	9.3	3.5	6.9
<i>O. dalli</i>	16.136	G-158463	-20.1	1.5	45.3	16.2	3.3	7.6
<i>O. dalli</i>	16.137	G-166790	-20.3	1.5	43.6	15.9	3.2	17.1
<i>O. dalli</i>	16.139	G-158389	-21.7	3.7	49.8	17.6	3.3	6.5
<i>O. dalli</i>	16.140	G-158464	-20.3	1.9	45.3	15.8	3.3	7.6
n			6	6				
Mean			-20.6	2.1				
SD			0.8	0.9				

^aUSR1 bone collagen isotope values are averages of two aliquots from the same collagen extraction run on separate days, as follows: aliquot-1 ($\delta^{13}\text{C} = -18.40\text{\textperthousand}$, $\delta^{15}\text{N} = 9.16\text{\textperthousand}$) and aliquot-2 ($\delta^{13}\text{C} = -18.45\text{\textperthousand}$, $\delta^{15}\text{N} = 9.07\text{\textperthousand}$).

^b Results first reported in Halffman et al., 2015 (34).

Table S3. Primers used in this study, with coordinates, targeted species, and annealing temperatures.

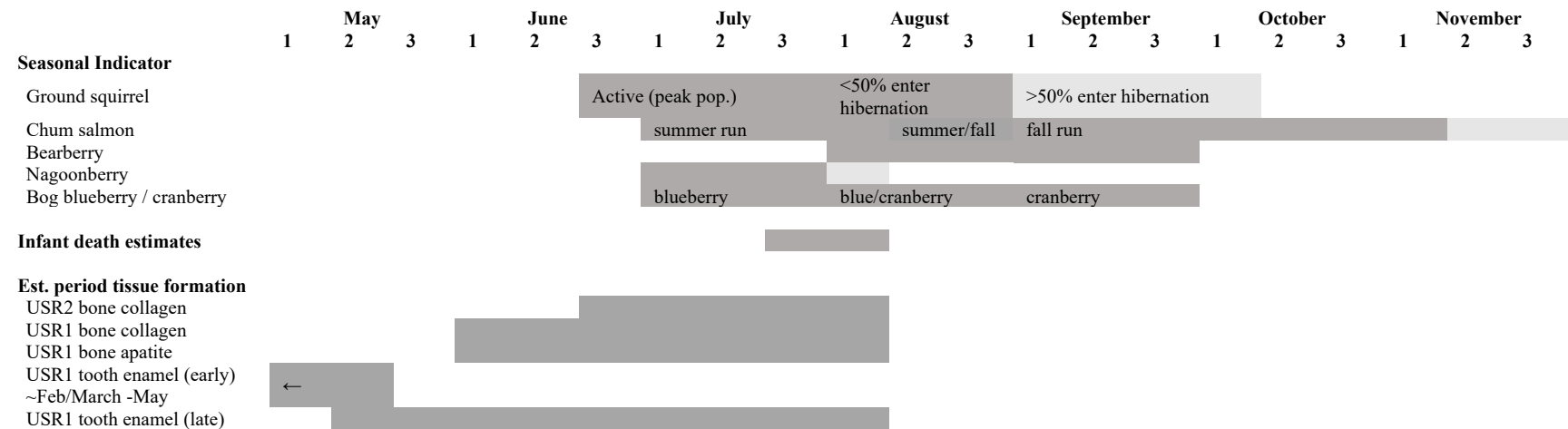
Target Region	Primer	Reference Sequence	Coordinates to mtDNA	Sequence (5' to 3')	Amplicon Length	Species Targeted	Annealing Temperature
CytB	BisonAF	<i>Bison priscus</i> KM593920.1	14660-14680	TATTCCTAGCAATACACTACA	131	<i>Bison priscus</i>	56°C
	BisonAR1		14770-14790	GATAAAGAATATTGAAGCTCC			
CytB	BisonAF	<i>Bison priscus</i> KM593920.1	14660-14680	TATTCCTAGCAATACACTACA	163	<i>Bison priscus</i>	56°C
	BisonAR2		14804-14822	TATAGGCCTCGTCCCTACGT			
CytB	BisonBF	<i>Bison priscus</i> KM593920.1	14720-14739	TCTGCCGAGACGTGAAC TAC	144	<i>Bison priscus</i>	62°C
	BisonBR1		14841-14863	CTCCAATATTCATGTTCTAGG			
CytB	BisonBF	<i>Bison priscus</i> KM593920.1	14720-14739	TCTGCCGAGACGTGAAC TAC	183	<i>Bison priscus</i>	62°C
	BisonBR2		14880-14902	CTATGAATGCTGTAGCTATTACT			
COI	ElkCOIF	<i>Cervus canadensis</i> JF443209.1	100-121	GACGACCAAATTATAATGTTA	163	<i>Cervus canadensis</i>	56°C
	ElkCOIR		240-262	GTAAAAGCTTATATTGTTTATT			
CytB	ElkCytbF	<i>Cervus canadensis</i> AB021096.1	50-69	CATTATTGACCTCCCAGCC	170	<i>Cervus canadensis</i>	60°C
	ElkCytbR		200-219	GACATCTGACAGATATGGG			
COI	Art1F	<i>Rangifer tarandus</i> KM506758.1	5517-5540	AATAATTCTTTATAGTAATGCC	196	<i>Alces alces</i> <i>Bison priscus</i> <i>Cervus canadensis</i> <i>Ovis dalli</i> <i>Rangifer tarandus</i>	58°C
	Art1R		5690-5712	GTATACRGTTCARCCTGTTCTG			
COI	Art2F	<i>Rangifer tarandus</i> KM506758.1	5821-5843	ACAACAATTATTAAYATAAAACC	173	<i>Alces alces</i> <i>Bison priscus</i> <i>Cervus canadensis</i> <i>Ovis dalli</i> <i>Rangifer tarandus</i>	54°C
	Art2R		5969-5993	GCTGGGT CRAARAAG GTTGATT			
COI	Art3F	<i>Rangifer tarandus</i> KM506758.1	5566-5588	TGACTWGTT CCTCTAATAATTGG	186	<i>Alces alces</i> <i>Bison priscus</i> <i>Cervus canadensis</i> <i>Ovis dalli</i> <i>Rangifer tarandus</i>	62°C
	Art3R		5732-5751	TGARGCTCCTGCRTGRGCTA			
12S	OST12-F	<i>Oncorhynchus mykiss</i> DQ288271.1	572-591	GCTTAAAACCCAAAGGACTTG	189	Salmonids	55°C
	OST12-R		741-760	CTACACCTCGACCTGACGTT			

Table S4. DNA results. Amplification is indicated by check marks (✓) with the corresponding number of replicates in parentheses, where applicable. Amplification failure is indicated with an o symbol. Sequence read length and mutations relative to reference sequence are notes.

ID	Primers	Amplification	Sequence Read	Mutations	GenBank Accession Number
Bison					
16.179	BisonAF/R1	✓ (2)	14,681-14,743	14,713C	MN931661
	BisonAF/R2	O			
	BisonBF/R1	O			
	BisonBF/R2	O			
	Art1F/R	O			
	Art2F/R	O			
	Art3F/R	O			
	BisonAF/R1	✓	14,681-14,766	14,713C	MN931662
16.180	BisonAF/R2	O			
	BisonBF/R1	O			
	BisonBF/R2	✓ (2)	14,740-14,879	Reference	MN931663
	Art1F/R	O			
	Art2F/R	O			
	Art3F/R	✓ (2)	5,945-6,093	6,046C	MN931671
	BisonAF/R1	✓	14,681-14,769	14,713C	MN931664
	BisonAF/R2	✓ (3)	14,681-14,801	14,713C	MN931665
16.181	BisonBF/R1	O			
	BisonBF/R2	✓	14,740-14,879	Reference	MN931666
	Art1F/R	O			
	Art2F/R	O			
	Art3F/R	✓	5,943-6,087	6,046C	MN931672
	BisonAF/R1	✓ (4)	14,681-14,769	14,713C	MN931667
	BisonAF/R2	O			
	BisonBF/R1	O			
16.182	BisonBF/R2	O			
	Art1F/R	O			
	Art2F/R	O			
	Art3F/R	O			

ID	Primers	Amplification	Sequence Read	Mutations	GenBank Accession Number
16.184	BisonAF/R1	✓ (2)	14,681-14,769	14,713C	MN931668
	BisonAF/R2	O			
	BisonBF/R1	O			
	BisonBF/R2	O			
	Art1F/R	O			
	Art2F/R	O			
	Art3F/R	O			
17.276	BisonAF/R1	✓ (2)	14,681-14,769	14,713C	MN931669
	BisonAF/R2	✓	14,681-14,803	14,713C	MN931670
	BisonBF/R1	O			
	BisonBF/R2	O			
	Art1F/R	O			
	Art2F/R	O			
	Art3F/R	O			
Caribou†					
17.284	Art1F/R	O			
	Art2F/R	O			
	Art3F/R	✓	5,589-5,731	Reference	MN931673
Salmon‡					
15.301	OST12-F/R	✓ (5)	593-740	660T, 713T	MN931677
16.109	OST12-F/R	✓ (5)	593-740	660T, 713T	MN931678
17.106	OST12-F/R	✓ (4)	593-740	660T, 713T	MN931679
17.109	OST12-F/R	✓ (3)	593-740	660T, 668delT, 713T	MN931680
17.110	OST12-F/R	✓ (2)	593-740	660T, 668delT, 713T	MN931681
17.111	OST12-F/R	✓	593-740	660T, 668delT, 713T	MN931682
17.112	OST12-F/R	✓ (6)	593-740	660T, 668delT, 713T	MN931683
Elk§					
16.171	ELKCytBF/R	O			
	ELKCOIF/R	✓	122-239	Reference	MN931674
16.175	ELKCytBF/R	O			
	ELKCOIF/R	✓	122-239	Reference	MN931675
16.176	ELKCytBF/R	O			
	ELKCOIF/R	✓	122-239	Reference	MN931676

Table S5. Seasonality indicators at Upward Sun River Component 3.



Notes. References: arctic ground squirrel phenology (88, 89); chum salmon migration and spawning (28); berry ripening and harvest (87, 91). Shading for bone collagen and bone apatite formation indicates the estimated period over which ~70% of the tissue was formed. Estimates are based on new models of fetal bone turnover rates presented here (Tables S6–S7) and previously-published estimates of postnatal bone tissue turnover rate (15) and assume that USR1 died at ~3 postnatal weeks (based on the uncertainty overlap between osteometric and dental age point estimates) and USR2 died at 33 gestational weeks (5). Estimated period of enamel formation assumes that enamel formation for the deciduous maxillary lateral incisor begins around 17 gestational weeks (27).

Table S6. Weekly bone collagen and mineral turnover, remodeling, and modeling rates by gestational age (weeks).

Age (weeks)	Turnover rate		Remodeling rate		Modeling rate	
	Collagen	Mineral	Collagen	Mineral	Collagen	Mineral
Gestational						
28	0.247	NA	0.149	NA	0.111	0.116
29	0.241	NA	0.142	NA	0.111	0.116
30	0.235	NA	0.136	NA	0.111	0.116
31	0.229	NA	0.129	NA	0.111	0.116
32	0.223	0.220	0.122	0.117	0.111	0.116
33	0.217	0.214	0.115	0.111	0.111	0.116
34	0.211	0.208	0.108	0.104	0.111	0.116
35	0.205	0.203	0.101	0.098	0.111	0.116
36	0.198	0.197	0.095	0.092	0.111	0.116
37	0.192	0.191	0.088	0.085	0.111	0.116
38	0.186	0.186	0.081	0.079	0.111	0.116
39	0.180	0.180	0.074	0.072	0.111	0.116
40	0.174	0.174	0.067	0.066	0.111	0.116
41	0.168	0.169	0.061	0.060	0.111	0.116
42	0.162	0.163	0.054	0.053	0.111	0.116
Postnatal						
0–3	0.104	0.084				
0–6	0.207	0.167				

Table S7. Proportion of total bone collagen and mineral formed by week at specified gestational and postnatal ages. Shown are ages 33 gestational weeks (GW) (estimated age of USR2), 40 GW (Newborn), and 3 postnatal weeks (PW) (USR1 age estimate based on uncertainty overlap between osteometric and dental age point estimates).

Week of tissue formation	Proportion of total tissue					
	33 GW		40 GW		3 PW	
	Collagen	Mineral	Collagen	Mineral	Collagen	Mineral
Gestational						
28 ^a	0.275	NA	0.063	NA	0.056	NA
29	0.087	NA	0.020	NA	0.018	NA
30	0.110	NA	0.025	NA	0.023	NA
31	0.139	NA	0.032	NA	0.028	NA
32 ^b	0.173	0.786	0.040	0.178	0.036	0.163
33	0.215	0.214	0.049	0.048	0.044	0.044
34			0.060	0.059	0.054	0.054
35			0.073	0.073	0.066	0.066
36			0.088	0.088	0.079	0.080
37			0.106	0.105	0.095	0.097
38			0.125	0.126	0.112	0.115
39			0.147	0.149	0.132	0.136
40			0.172	0.174	0.154	0.160
Postnatal						
0–3					0.104	0.084

^aFor collagen, gestational week 28 includes the proportion of collagen formed prior to and through the 28th week.

^bFor mineral, gestational week 32 includes the proportion of mineral formed prior to and through the 32nd week.

Table S8 Inputs for 5-source (bison, salmon, small game, wapiti, and whitefish), 2-biotracer ($\delta^{13}\text{C}_{\text{collagen}}$ and $\delta^{15}\text{N}_{\text{collagen}}$) MixSIAR model. Isotope values and collagen-to-collagen, source-to-consumer trophic discrimination factors ($\Delta^{13}\text{C}$ and $\Delta^{15}\text{N}$) are shown as the mean and standard deviation (in parentheses).

	$\delta^{13}\text{C} (\text{\textperthousand})$	$\delta^{15}\text{N} (\text{\textperthousand})$	n	$\Delta^{13}\text{C} (\text{\textperthousand})$	$\Delta^{15}\text{N} (\text{\textperthousand})$
USR1	-18.4	9.1			
USR2	-18.4	8.7			
Bison	-21.5 (0.4)	4.7 (1.4)	10	1.1 (0.2)	3.8 (1.1)
Salmon	-15.9 (0.4)	11.3 (1.0)	7	1.1 (0.2)	3.8 (1.1)
Small Game	-21.5 (0.9)	1.1 (0.7)	16	1.1 (0.2)	3.8 (1.1)
Wapiti	-20.7 (0.6)	2.1 (.9)	16	1.1 (0.2)	3.8 (1.1)
Whitefish	-24.6 (0.9)	9.9 (0.8)	5	1.1 (0.2)	3.8 (1.1)

Table S9. Estimated food source contributions to maternal diets. Results are based on a 5-source (bison, salmon, small game, wapiti, and whitefish), 2-biotracer ($\delta^{13}\text{C}_{\text{collagen}}$ and $\delta^{15}\text{N}_{\text{collagen}}$) mixing model in MixSIAR. Small game is an *a priori* aggregation of ground squirrel, grouse/ptarmigan, and hare. Results are shown for both unaggregated and *a posteriori* aggregated terrestrial sources. Lower (LC95) and upper (UC95) bounds of the 95% credible interval are defined, respectively, as the 0.025 quantile and the 0.975 quantile of the posterior probability distribution.

Source	Contribution to Diet (%)							
	USR1				USR2			
	Mean	sd	LC95	UC95	Mean	sd	LC95	UC95
Terrestrial (Aggregated)	62	8	47	77	65	8	50	80
Salmon	32	6	20	44	30	7	16	42
Whitefish	6	5	0	17	5	4	0	16
Unaggregated terrestrial								
Bison	16	13	1	45	15	12	1	45
Small Game	21	14	1	52	23	15	1	54
Wapiti	25	16	1	59	27	17	1	62

Table S10. Mixing model sensitivity to varied nitrogen isotope discrimination factors ($\Delta^{15}\text{N}$). Results are based on a 5-source (bison, salmon, small game, wapiti, and whitefish), 2-biotracer ($\delta^{13}\text{C}_{\text{collagen}}$ and $\delta^{15}\text{N}_{\text{collagen}}$) mixing model in MixSIAR. Terrestrial is an *a posteriori* aggregation of bison, wapiti, and small game. $\Delta^{13}\text{C}=1.1 \pm 0.2\text{\textperthousand}$ for all models. Main model appears in bold ($\Delta^{15}\text{N}=3.8\text{\textperthousand}$).

Model $\Delta^{15}\text{N}$ (%)	Estimated Mean Contribution ± 1 SD (%)		
	Terrestrial	Salmon	Whitefish
USR1			
$\Delta^{15}\text{N} = 2.8$	56 \pm 9	36 \pm 6	8 \pm 6
$\Delta^{15}\text{N} = 3.8$	62 \pm 8	32 \pm 6	6 \pm 5
$\Delta^{15}\text{N} = 4.8$	69 \pm 8	27 \pm 7	4 \pm 4
$\Delta^{15}\text{N} = 5.8$	75 \pm 8	21 \pm 7	3 \pm 3
USR2			
$\Delta^{15}\text{N} = 2.8$	58 \pm 8	34 \pm 6	7 \pm 6
$\Delta^{15}\text{N} = 3.8$	65 \pm 8	30 \pm 7	5 \pm 4
$\Delta^{15}\text{N} = 4.8$	71 \pm 8	25 \pm 7	4 \pm 4
$\Delta^{15}\text{N} = 5.8$	78 \pm 8	18 \pm 8	3 \pm 3

Table S11. Single essential amino acid $\delta^{13}\text{C}$ values for USR infants. Amino acids were isolated from bone collagen. All samples were run in triplicate and isotope values are reported as means \pm 1 standard deviation.

Amino Acid	$\delta^{13}\text{C}$ (‰ vs. VPDB)	
	USR1	USR2
Isoleucine (Ile)	-20.5 \pm 0.2	-21.3 \pm 0.2
Leucine (Leu)	-27.9 \pm 0.2	-28.2 \pm 0.2
Lysine (Lys)	-19.0 \pm 0.4	-19.5 \pm 0.5
Phenylalanine (Phe)	-25.4 \pm 0.8	-26.7 \pm 0.2
Threonine (Thr)	-7.2 \pm 0.2	-9.4 \pm 0.2
Valine (Val)	-23.6 \pm 0.2	-24.4 \pm 0.2

Table S12. EAA $\delta^{13}\text{C}$ dietary markers for the USR infants compared to archaeological terrestrial, marine, and freshwater protein consumers. Comparative consumer EAA $\delta^{13}\text{C}$ dietary markers were calculated using previously published data on bone collagen EAA carbon isotopic composition. $\Delta^{13}\text{C}_{\text{Val-Phe}} = \delta^{13}\text{C}_{\text{valine}} - \delta^{13}\text{C}_{\text{phenylalanine}}$ and $\Delta^{13}\text{C}_{\text{Lys-Phe}} = \delta^{13}\text{C}_{\text{lysine}} - \delta^{13}\text{C}_{\text{phenylalanine}}$. Values are also shown for modern major aquatic primary producers (algae) and terrestrial primary producers (plants) and were calculated using previously published data. Herbivores include only wild taxa. Marine mammals include only piscivorous taxa. Characterizations of human diets follow those of the original studies based on artifactual, zooarchaeological, locational, and/or isotopic evidence and indicate high, though not exclusive, consumption of a particular protein source.

Group	Orig. Study ID	Location	$\Delta^{13}\text{C}_{\text{Lys-Phe}} (\text{\textperthousand})$	$\Delta^{13}\text{C}_{\text{Val-Phe}} (\text{\textperthousand})$	Ref
Consumers (Archaeological)					
USR humans					
USR1	14.801		6.4	1.8	This study
USR2	15.201		7.2	2.3	This study
Freshwater protein consumers					
Human	IG1	Serbia	6.6	5.6	(18)
Human	IG2	Serbia	7.1	6.7	(18)
Human	IG3	Serbia	7.9	7.3	(18)
Human	IG4	Serbia	7.0	6.9	(18)
Human	IG5	Serbia	7.3	6.8	(18)
Human	IG6	Serbia	7.0	6.8	(18)
Human	IG7	Serbia	7.2	6.7	(18)
Human	IG16	Serbia	7.2	7.2	(18)
Human	IG17	Serbia	6.9	6.9	(18)
Human	IG18	Serbia	8.2	7.1	(18)
Marine protein consumers					
Sea lion	SEVA-1721	South Korea	8.0	3.6	(72)
Dolphin	SEVA-3918	South Korea	7.6	3.1	(72)
Sea lion	SEVA-3920	South Korea	7.2	3.3	(72)
Sea lion	SEVA-3931	South Korea	8.0	4.2	(72)
Seal	J2	Japan	8.7	4.7	(18)
Seal	J8	Japan	8.5	3.8	(18)
Seal	KOP129	Sweden	7.2	5.3	(74)
Porpoise	KOP166	Sweden	6.9	4.1	(74)
Porpoise	KOP167	Sweden	7.3	3.2	(74)
Seal	KOP180	Sweden	7.4	1.6	(74)
Seal	KOP97	Sweden	7.9	4.1	(74)
Seal	KOP98	Sweden	7.6	5.0	(74)
Human	J1	Japan	7.9	4.6	(18)
Human	J4	Japan	8.1	4.8	(18)
Human	J5	Japan	8.5	4.2	(18)
Human	Indiv 1	Greenland	8.3	6.6	(73)
Human	Indiv 2	Greenland	8.2	6.5	(73)
Human	Indiv 3	Greenland	8.0	5.0	(73)
Human	Indiv 4	Greenland	8.3	6.1	(73)
Human	Indiv 5	Greenland	8.3	6.6	(73)
Human	Indiv 6	Greenland	9.0	6.8	(73)
Terrestrial protein consumers					
Deer	SEVA-1732	South Korea	5.7	-1.6	(72)

Group	Orig. Study ID	Location	$\Delta^{13}\text{C}_{\text{Lys-Phe}} (\text{\textperthousand})$	$\Delta^{13}\text{C}_{\text{Val-Phe}} (\text{\textperthousand})$	Ref
Deer	SEVA-1905	South Korea	6.3	-0.7	(72)
Deer	SEVA-1907	South Korea	5.4	-2.9	(72)
Deer	SEVA-1929	South Korea	5.5	-1.9	(72)
Deer	D11-1-D	Bulgaria	5.9	-0.2	(18)
Deer	IG10-D	Serbia	5.8	-0.9	(18)
Deer	IG23-D	Serbia	5.5	-0.5	(18)
Deer	IG8-D	Serbia	4.9	-1.3	(18)
Deer	J6-D	Japan	6.5	-0.1	(18)
Deer	J7-D	Japan	6.0	-0.7	(18)
Moose	AZV56	Latvia	6.1	-1.6	(19)
Moose	KOP142	Sweden	6.0	-2.8	(74)
Moose	KOP162	Sweden	6.5	-1.4	(74)
Hare	ROSS36	Sweden	5.4	-1.4	(74)
Terrestrial protein (C ₃) consumers					
Human	D193	Bulgaria	5.1	1.3	(18)
Human	D596	Bulgaria	5.0	0.4	(18)
Human	D706	Bulgaria	5.0	1.0	(18)
Human	D772	Bulgaria	4.8	0.7	(18)
Human	D898	Bulgaria	4.5	0.0	(18)
Human	IG11	Serbia	4.0	0.9	(18)
Human	IG12	Serbia	3.4	0.5	(18)
Human	IG13	Serbia	4.0	0.7	(18)
Human	IG14	Serbia	4.0	0.4	(18)
Human	IG15	Serbia	4.5	1.4	(18)
Human	V11	Bulgaria	5.3	1.0	(18)
Human	V32	Bulgaria	5.4	0.9	(18)
Human	V43	Bulgaria	5.8	1.0	(18)
Human	ROSS05	Sweden	5.1	1.5	(74)
Human	ROSS06	Sweden	3.9	1.0	(74)
Human	ROSS08	Sweden	4.7	-0.2	(74)
Human	ROSS09	Sweden	4.5	-0.2	(74)
Human	ROSS10	Sweden	4.8	-0.3	(74)
Human	ROSS13	Sweden	3.3	-0.8	(74)
Human	ROSS15	Sweden	5.2	0.0	(74)
Human	ROSS16	Sweden	4.0	-1.1	(74)
Human	ROSS18	Sweden	3.0	-0.7	(74)
Human	ROSS20	Sweden	3.6	-1.4	(74)
Terrestrial protein (C ₄) consumers					
Human	M1	Belize	2.6	-0.6	(18)
Human	M2	Belize	2.6	0.0	(18)
Human	M3	Belize	4.0	-0.4	(18)
Human	M4	Belize	3.6	-0.3	(18)
Human	M5	Belize	2.5	0.2	(18)
Human	M6	Belize	2.4	-0.1	(18)
Human	M7	Belize	2.3	0.2	(18)
Human	M8	Belize	2.4	0.2	(18)
Human	M9	Belize	2.9	-0.2	(18)
Human	M10	Belize	2.9	1.8	(18)
Human	M11	Belize	2.5	-0.2	(18)

Group	Orig. Study ID	Location	$\Delta^{13}\text{C}_{\text{Lys-Phe}} (\text{\textperthousand})$	$\Delta^{13}\text{C}_{\text{Val-Phe}} (\text{\textperthousand})$	Ref
Human	M12	Belize	2.7	0.1	(18)
Human	M14	Guatemala	2.3	0.7	(18)
Human	M15	Guatemala	2.1	0.4	(18)
Primary producers					
Algae					
Microalgae	C1	Lab culture	6.9	0.9	(17)
Microalgae	C2	Lab culture	10.8	1.8	(17)
Microalgae	C3	Lab culture	6.4	-0.7	(17)
Microalgae	C4	Lab culture	10.2	-0.2	(17)
Microalgae	D1	Lab culture	9.3	4.3	(17)
Microalgae	D2	Lab culture	8.5	2.8	(17)
Microalgae	D3	Lab culture	4.8	0.9	(17)
Microalgae	D4	Lab culture	8.6	0.9	(17)
Microalgae	D5	Lab culture	7.5	0.5	(17)
Microalgae	H1	Lab culture	7.5	-1.7	(17)
Microalgae	H2	Lab culture	10.1	3.5	(17)
Microalgae	H3	Lab culture	9.6	-1.8	(17)
Microalgae	H4	Lab culture	9.6	2.8	(17)
Microalgae	K1	Lab culture	6.7	0.5	(17)
Microalgae	K2	Lab culture	9.2	0.8	(17)
Microalgae	K3	Lab culture	10.7	2.9	(17)
Microalgae	K4	Lab culture	8.0	0.4	(17)
Microalgae	K5	Lab culture	8.3	1.8	(17)
Microalgae	K6	Lab culture	7.9	2.5	(17)
Microalgae	N1	Kiel fjord	8.9	0.6	(17)
Microalgae	N2	Kiel fjord	8.8	-0.4	(17)
Microalgae	N3	Kiel fjord	9.0	-0.2	(17)
Macroalgae	P1	California	8.3	0.6	(17)
Macroalgae	P2	California	10.0	2.1	(17)
Macroalgae	P3	California	9.5	1.5	(17)
Macroalgae	P4	California	9.0	3.2	(17)
Macroalgae	P5	California	9.8	1.4	(17)
Macroalgae	P6	California	11.1	2.4	(17)
Macroalgae	P7	California	9.6	-0.3	(17)
Macroalgae	P8	California	9.7	0.8	(17)
Macroalgae	P9	California	8.5	2.2	(17)
Macroalgae	P10	California	12.8	2.4	(17)
Macroalgae	P11	California	8.2	1.8	(17)
Macroalgae	P12	California	12.1	-1.2	(17)
Macroalgae	R1	California	8.3	0.0	(17)
Macroalgae	R2	California	7.7	-0.6	(17)
Macroalgae	R3	California	8.9	-0.1	(17)
Macroalgae	R4	California	8.8	3.9	(17)
Macroalgae	R5	California	8.9	2.9	(17)
Macroalgae	R6	California	8.0	0.4	(17)
Macroalgae	R7	California	10.1	0.8	(17)
Macroalgae	R8	California	6.2	-1.6	(17)
Macroalgae	R9	California	9.2	1.6	(17)
Microalgae	X1	Lab culture	11.2	1.7	(17)

Group	Orig. Study ID	Location	$\Delta^{13}\text{C}_{\text{Lys-Phe}} (\text{\textperthousand})$	$\Delta^{13}\text{C}_{\text{Val-Phe}} (\text{\textperthousand})$	Ref
Microalgae	X2	Lab culture	10.8	2.0	(17)
Microalgae	X3	Lab culture	9.1	1.6	(17)
Microalgae	X4	Lab culture	9.9	1.7	(17)
Microalgae	Y1	Lab culture	8.1	2.4	(17)
Plants					
<i>Quercus robur</i>	T1	Denmark	6.9	-4.6	(17)
<i>Alnus glutinosa</i>	T2	Denmark	6.0	-2.2	(17)
<i>Salix</i> sp.	T3	Alaska	4.5	-4.4	(17)
<i>Polygonum viviparum</i>	T4	Alaska	4.9	-4.5	(17)
<i>Carex aquatilis</i>	T5	Alaska	5.2	-3.9	(17)
<i>Calamagrostis canadensis</i>	T6	Alaska	4.0	-3.1	(17)
<i>Menyanthes trifoliata</i>	T7	Alaska	5.2	-3.5	(17)
<i>Betula nana</i>	T8	Alaska	3.9	-2.8	(17)
<i>Carex utriculata</i>	T9	Alaska	4.6	-3.7	(17)
<i>Salix reticulata</i>	T10	Alaska	3.2	-4.1	(17)
<i>Eriophorum angustifolium</i>	T11	Alaska	5.2	-3.0	(17)
<i>Rumex arcticus</i>	T12	Alaska	4.3	-4.2	(17)

Table S13. Faunal ubiquity (n = 16 sites between 13,000-10,000 cal yr BP. Data from Potter et al. (30).

TAXON	COMMON NAME	MASS (KG)	N OF OCCURRENCES	% OF SITES
<i>Ungulates</i>				
<i>Bison priscus</i>	Steppe bison	360-907	9	56
<i>Cervus canadensis</i>	Elk/wapiti	171-497	5	31
<i>Rangifer tarandus</i>	Caribou	63-153	3	19
<i>Ovis dalli</i>	Dall's sheep	46-110	3	19
<i>Alces alces</i>	Moose	200-600	1	6
<i>Small mammals</i>				
<i>Urocitellus parryi</i>	Ground squirrel	<1	4	25
<i>Lepus</i> sp.	Hare	1-2	3	19
<i>Marmota</i> sp.	Marmot	3-6	2	13
<i>Carnivores</i>				
<i>Ursus</i> sp.	Bear	92-270 Black 100-600 brown	2	13
Canidae	Canids	3-80	2	13
<i>Other</i>				
Aves (terrestrial or waterfowl)	Birds	<1-17	7	44
Pisces	Fish	<1-23	4	25

Table S14. Faunal NISP summaries of likely food sources from three middle Tanana basin residential sites. Excludes carnivores and small rodents.

	Broken Mammoth CZ3 [fall, early --winter] 12,386–11,769 cal yr BP (33)	Mead CZ3 [season unknown] 12,671–12,142 cal yr BP (30)	USR C3 [summer] 11,600–11,230 cal yr BP (30)
Large/Very Large Mammals			
<i>Bison</i> sp. (bison)	133	10	
<i>Cervus canadensis</i> (wapiti)	87	--	
<i>Rangifer tarandus</i> (caribou)	6	--	
<i>Alces alces</i> (moose)	4	1	
<i>Ovis dalli</i> (Dall's sheep)	11	--	
Unidentified L/VL mammal	639	14	*
Small/Medium Mammals			
<i>Lepus</i> sp. (hare)	33	1	48
<i>Marmota</i> sp. (marmot)	8	--	4
<i>Urocitellus parryi</i> (ground squirrel)	298	--	242
Unidentified S/M mammal	108	4	*
Birds			
Anatidae and Gruidae (waterfowl)	74	4	--
Tetraoninae (ptarmigan/grouse)	22	--	16
Unidentified/other Aves	117	1	12
Fish			
<i>Oncorhynchus</i> sp. (salmon)	--	--	362
Unidentified fish	28	1	25

* At USR, several hundred bone fragments were classed as L mammal (e.g., caribou or sheep) to VL mammal (e.g., bison, wapiti, or moose).

Table S15. Estimated source contributions to USR C3 hearth sediments. Results are adapted from Choy et al. (31) (their table S8) based on their 3-source (terrestrial, freshwater, and marine), 3-biotracer ($\delta^{15}\text{N}_{\text{bulk}}$, $\delta^{13}\text{C}_{16:0}$ and $\delta^{13}\text{C}_{18:0}$) mixing model in SIAR.

Hearth	N samples	Mean Contribution (%)		
		Terrestrial	Freshwater	Marine (salmon)
F2010-1	1	75	20	5
F2010-5	2	72	20	9
F2011-6A	1	43	27	29
F2013-9	5	45	28	27
F2013-10	1	73	17	10
F2013-11	1	72	18	10
F2013-13	1	47	29	24
F2013-20	4	40	27	34
F2014-6	2	12	34	55
Mean hearth		53	24	22

Table S16. Internal standard reference materials used to calibrate bone collagen $\delta^{13}\text{C}$ relative to VPDB and $\delta^{15}\text{N}$ relative to AIR (Washington State University Stable Isotope Core Laboratory).

Internal Standard	Material	$\delta^{13}\text{C}$ (‰ vs. VPDB)	$\delta^{15}\text{N}$ (‰ vs. AIR)
G-7	Keratin	-23.70	6.06
G-16	Yeast	-10.14	0.08
G-55	Corn	-13.36	--
G-177	Acetanilide #5	-28.38	-0.63
G-199	Beef blood serum	-10.97	7.66
G-200	Glutamic acid	-27.20	-4.57

Notes. Internal standards were calibrated to the following internationally-certified standard reference materials: for $\delta^{13}\text{C}$, USGS40, USGS41a, USGS64, USGS66, NBS18, NBS19, and LSVEC, and, for $\delta^{15}\text{N}$, USGS40, USGS41a, USGS64, USGS66, USGS25, and USGS26. The G-55 internal standard calibration also included IAEACO-9, IAEA-CH-6 Sucrose, and USGS32. Sample carbon and nitrogen stable isotope compositions were calibrated to VPDB and AIR using internal standards G-199 and G-200, except for samples G-116714 through G-147962, which were calibrated to AIR using internal standards G-7 and G-177 and to VPDB using three standards (G-7, G-177, and either G-16 or G-55).

Table S17. Internal amino acid standards and their $\delta^{13}\text{C}$ values prior to derivatization (Alaska Stable Isotope Facility).

Internal Amino Acid Standard	Lot Number	$\delta^{13}\text{C}$ (‰ vs. VPDB)
L-Isoleucine	BCBD5312V	-11.2
L-Leucine	BCBM2322V	-28.9
L-Lysine	BCBR4746V	-27.3
L-Phenylalanine	SLBQ7928V	-12.1
L-Threonine	BCBM6174V	-10.5
L-Valine	BCBQ2367V	-10.9

Notes. All of the amino acid standards were purchased from Sigma Aldrich, St. Louis, MO, USA. The $\delta^{13}\text{C}$ of these amino acid standards, prior to derivatization, were determined via elemental analyzer (EA) attached to the isotope ratio mass spectrometer (Flash 2000 Organic EA connected via a Conflo IV to an IRMS (DeltaV Plus) at ASIF), which determined the $\delta^{13}\text{C}$ values relative to tank gas CO₂ (Bone Dry 3.0 Grade Carbon Dioxide, Size 200 Cylinder, CGA-320, Airgas Part #:CD BD200, Lot# 774000243203-1). The $\delta^{13}\text{C}$ value of the tank CO₂ is calibrated using a two-point calibration using two internationally-certified Standard Reference Materials (USGS 40 and USGS 41).

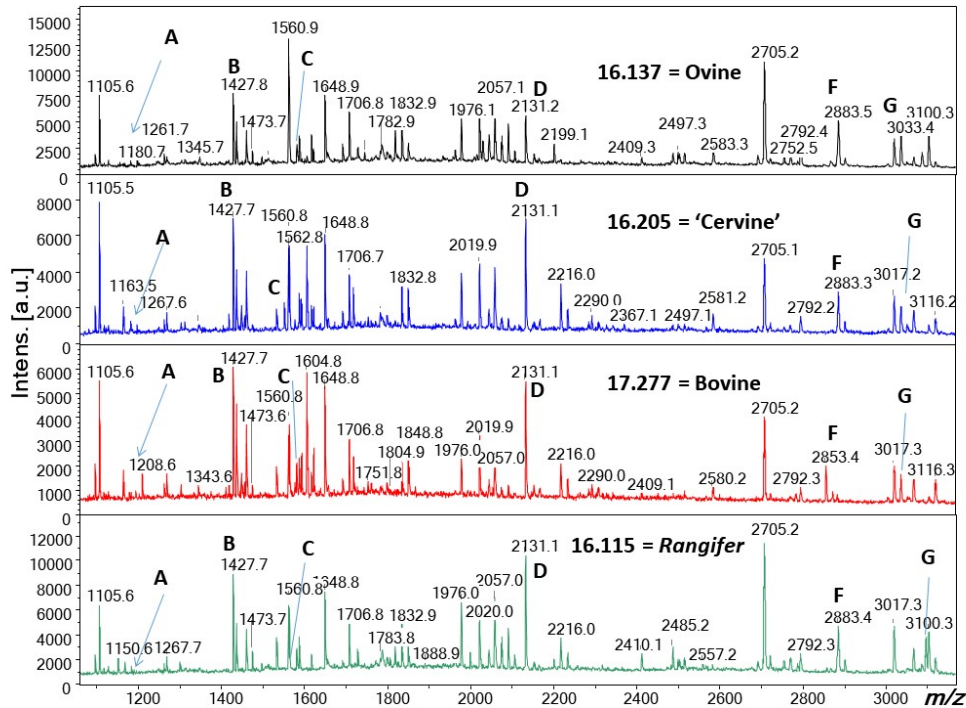


Fig. S1. Example collagen peptide mass fingerprint spectra of specimens identified (from top to bottom) as ovine, cervine, bovine, and *Rangifer*.

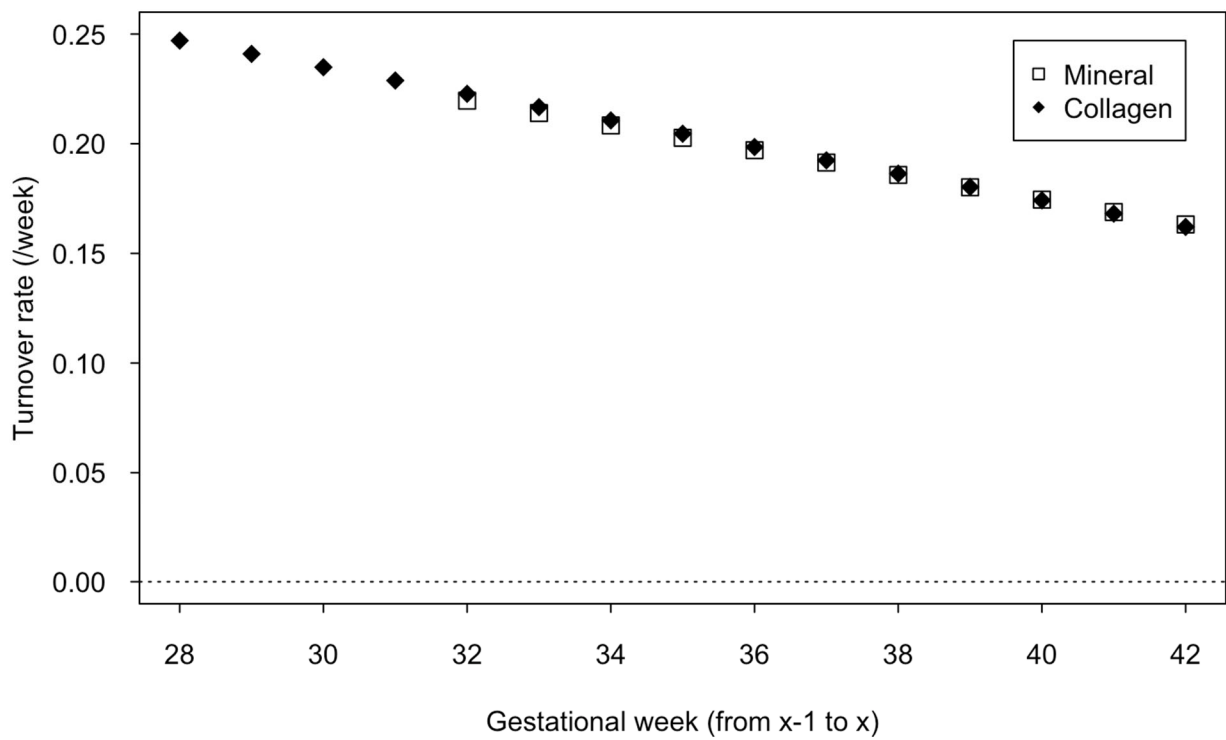


Fig. S2. Weekly bone collagen and mineral turnover rate by gestational age (weeks).

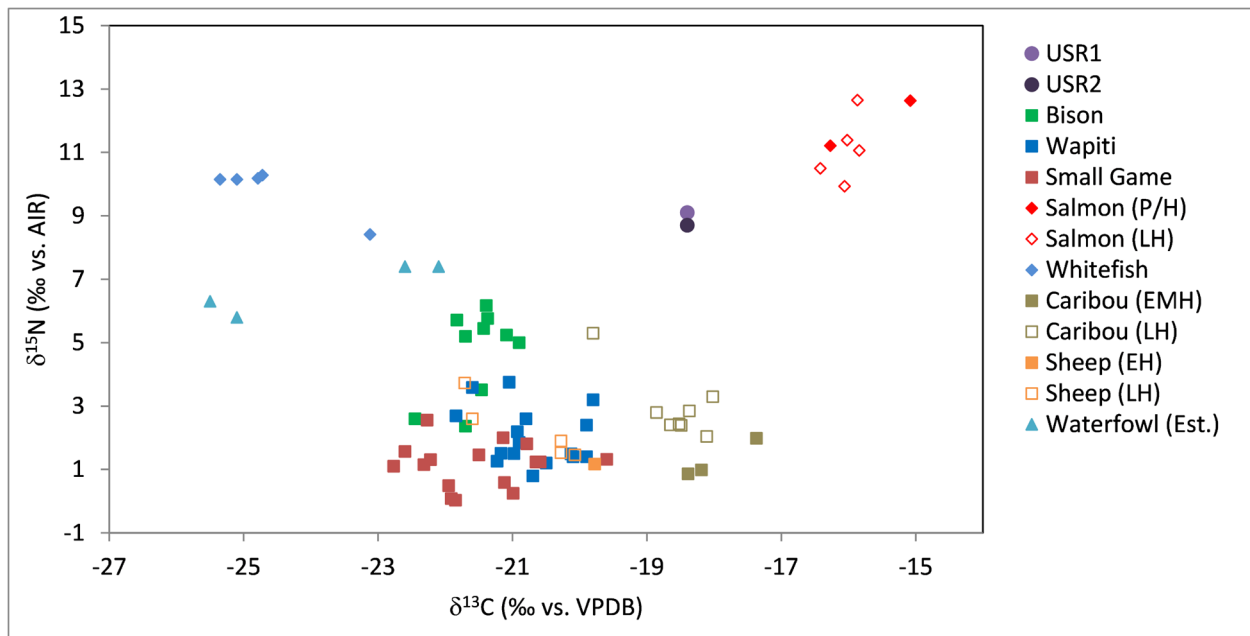


Fig. S3. Bone collagen $\delta^{13}\text{C}$ and $\delta^{15}\text{N}$ values for the USR infants and expanded potential food sources. Includes primary fauna (taxa present in USR C3 and/or ubiquitous in the regional faunal record for the terminal Pleistocene/early Holocene) and secondary fauna (not present in USR C3 but present in low frequencies in the regional faunal record for the terminal Pleistocene/early Holocene). Secondary fauna includes caribou, sheep, and waterfowl. Caribou, sheep, and salmon samples include early and recent specimens as indicated (P/H=terminal Pleistocene/early Holocene; EH=early Holocene; EMH=early to middle Holocene; LH=late Holocene). Small game is an average of hare, ground squirrel, and grouse/ptarmigan. Waterfowl (ducks and geese) $\delta^{13}\text{C}$ and $\delta^{15}\text{N}$ values are estimated from published modern muscle values (31), and their $\delta^{13}\text{C}$ values have been adjusted by +1.5‰ to account for the Suess effect (following the original publication) and an additional +2.4‰ to account for the collagen-muscle offset (75).

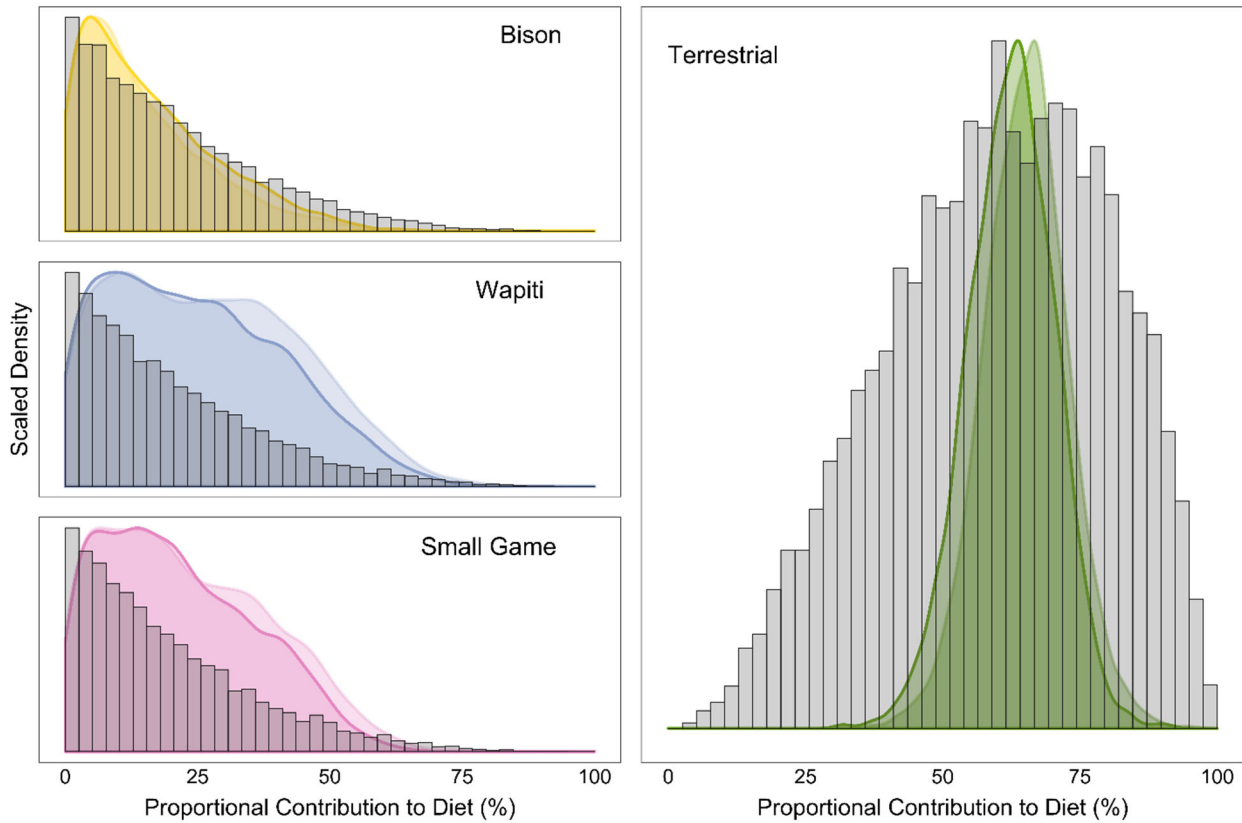


Fig. S4. Posterior distributions (colored) superimposed on prior distributions (gray) of discrete vs. aggregated terrestrial source contributions for USR1 (darker color) and USR2 (lighter color). Output is based on a 5-source (bison, wapiti, small game, salmon, and whitefish), 2-biotracer ($\delta^{13}\text{C}_{\text{collagen}}$ and $\delta^{15}\text{N}_{\text{collagen}}$) mixing model in MixSIAR. Small game is an *a priori* average of hare, ground squirrel, and grouse/ptarmigan. The posterior distributions for the aggregated terrestrial (an *a posteriori* aggregation of bison, wapiti, and small game) are narrow, peaked, and unimodal, and diverge from the prior distributions, indicating that the terrestrial contribution estimates are robust and informed by the isotope data (14, 16). However, for the individual terrestrial sources, the posterior distributions are broad and multimodal (wapiti and small game), or resemble the prior distribution (bison), indicating that the source contributions are confounded and cannot be resolved by the isotope data (14, 16).

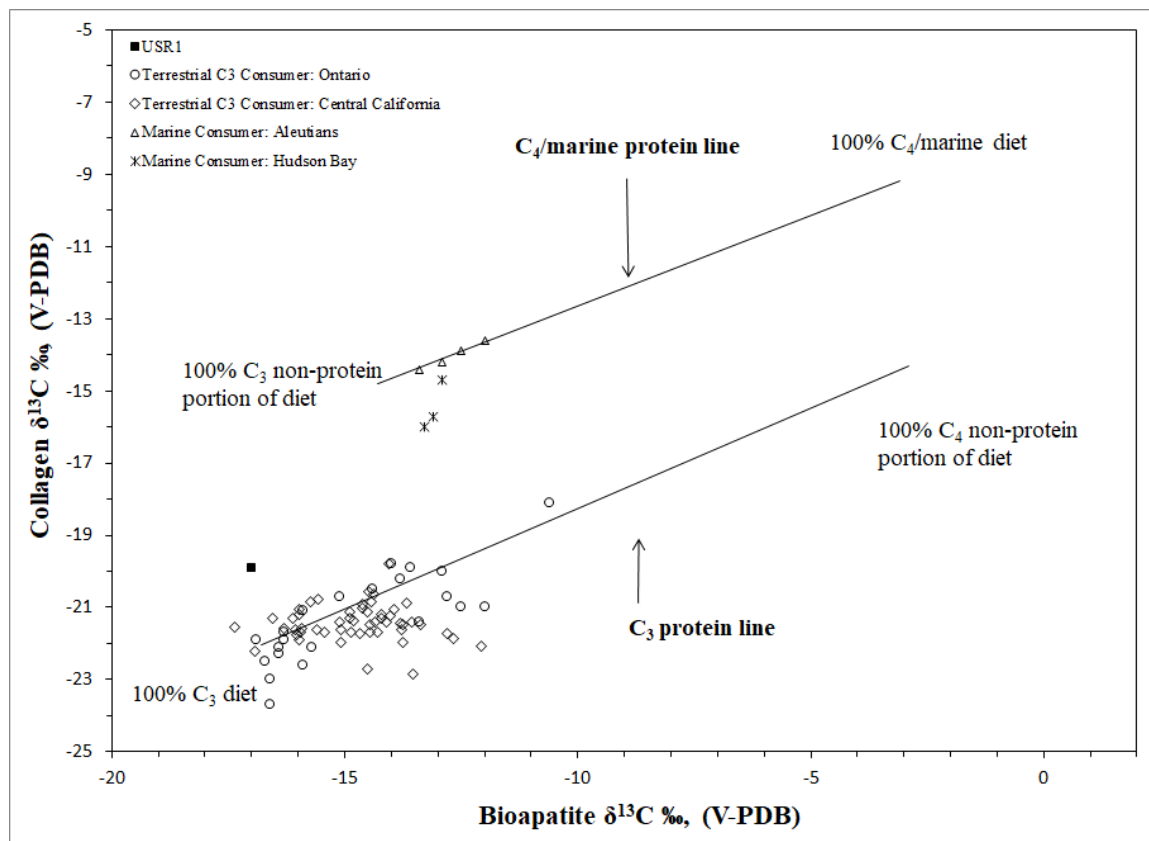


Fig. S5. $\delta^{13}\text{C}_{\text{collagen}}$ vs. $\delta^{13}\text{C}_{\text{bioapatite}}$ for USR1 compared to protein-source regression lines and prehistoric human groups with terrestrial or marine diets. Regression lines are based on experimental evidence from animals on known diets (following 22). $\delta^{13}\text{C}$ values for USR1 and other archaeological samples have been adjusted to account for the Suess effect by subtracting 1.5‰ from the measured values (for comparability with modern experimental animals) (22). Comparative archaeological human data are taken from published sources: (1) terrestrial C3 consumers-Ontario (108); terrestrial C3 consumers-central California (109); marine consumers (shown as means for various sites) (110).

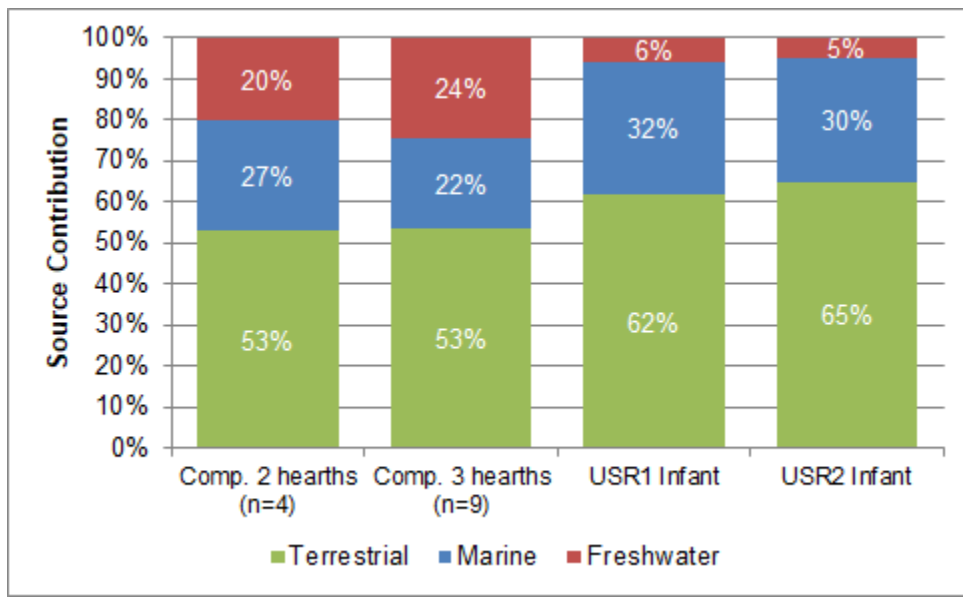


Fig. S6. Comparison of mixing model source proportional contribution estimates to USR hearth sediments versus USR infants. Hearth sediment results are adapted from Choy et al. (31) Table S8.

REFERENCES AND NOTES

1. T. A. Surovell, N. M. Waguespack, Human prey choice in the late Pleistocene and its relation to megafaunal extinctions, in *American Megafaunal Extinctions at the End of the Pleistocene*, G. Haynes, Ed. (Springer, 2009), pp. 77–105.
2. M. D. Cannon, D. J. Meltzer, Explaining variability in Early Paleoindian foraging. *Quat. Int.* **191**, 5–17 (2008).
3. E. J. Reitz, E. S. Wing, *Zooarchaeology* (Cambridge Univ. Press, 1999).
4. M. P. Richards, Isotope analysis for diet studies, in *Archaeological Science: An Introduction*, M. P. Richards, K. Britton, Eds. (Cambridge Univ. Press, 2020), pp. 125–143.
5. B. A. Potter, J. D. Irish, J. D. Reuther, H. J. McKinney, New insights into Eastern Beringian mortuary behavior: A terminal Pleistocene double infant burial at Upward Sun River. *Proc. Natl. Acad. Sci. U.S.A.* **111**, 17060–17065 (2014).
6. J. V. Moreno-Mayar, B. A. Potter, L. Vinner, M. Steinrücken, S. Rasmussen, J. Terhorst, J. A. Kamm, A. Albrechtsen, A.-S. Malaspina, M. Sikora, J. D. Reuther, J. D. Irish, R. S. Malhi, L. Orlando, Y. S. Song, R. Nielsen, D. J. Meltzer, E. Willerslev, Terminal Pleistocene Alaskan genome reveals first founding population of Native Americans. *Nature* **553**, 203–207 (2018).
7. J. C. Tackney, B. A. Potter, J. Raff, M. Powers, W. S. Watkins, D. Warner, J. D. Reuther, J. D. Irish, D. H. O'Rourke, Two contemporaneous mitogenomes from terminal Pleistocene burials in eastern Beringia. *Proc. Natl. Acad. Sci. U.S.A.* **112**, 13833–13838 (2015).
8. E. C. Webb, J. Lewis, A. Shain, E. Kastrisianaki-Guyton, N. V. Honch, A. Stewart, B. Miller, J. Tarlton, R. P. Evershed, The influence of varying proportions of terrestrial and marine dietary protein on the stable carbon-isotope compositions of pig tissues from a controlled feeding experiment. *Sci. Technol. Archaeolog. Res.* **3**, 28–44 (2017).
9. S. H. Ambrose, L. Norr, Experimental evidence for the relationship of the carbon isotope ratios of whole diet and dietary protein to those of bone collagen and carbonate, in *Prehistoric Human Bone*:

Archaeology at the Molecular Level, J. B. Lambert, G. Grupe, Eds. (Springer-Verlag, 1993), pp. 1–37.

10. M. P. Richards, S. Mays, B. T. Fuller, Stable carbon and nitrogen isotope values of bone and teeth reflect weaning age at the medieval Wharram Percy site, Yorkshire, UK. *Am. J. Phys. Anthropol.* **119**, 205–210 (2002).
11. B. T. Fuller, J. L. Fuller, D. A. Harris, R. E. M. Hedges, Detection of breastfeeding and weaning in modern human infants with carbon and nitrogen stable isotope ratios. *Am. J. Phys. Anthropol.* **129**, 279–293 (2006).
12. L. M. Reynard, N. Tuross, The known, the unknown and the unknowable: Weaning times from archaeological bones using nitrogen isotope ratios. *J. Archaeol. Sci.* **53**, 618–625 (2015).
13. D. L. Phillips, J. W. Gregg, Source partitioning using stable isotopes: Coping with too many sources. *Oecologia* **136**, 261–269 (2003).
14. B. C. Stock, A. L. Jackson, E. J. Ward, A. C. Parnell, D. L. Phillips, B. X. Semmens, Analyzing mixing systems using a new generation of Bayesian tracer mixing models. *PeerJ* **6**, e5096 (2018).
15. T. Tsutaya, M. Yoneda, Quantitative reconstruction of weaning ages in archaeological human populations using bone collagen nitrogen isotope ratios and approximate Bayesian computation. *PLOS ONE* **8**, e72327 (2013).
16. D. L. Phillips, R. Inger, S. Bearhop, A. L. Jackson, J. W. Moore, A. C. Parnell, B. X. Semmens, E. J. Ward, Best practices for use of stable isotope mixing models in food-web studies. *Can. J. Zool.* **92**, 823–835 (2014).
17. T. Larsen, M. Ventura, N. Andersen, D. M. O'Brien, U. Piatkowski, M. D. McCarthy, Tracing carbon sources through aquatic and terrestrial food webs using amino acid stable isotope fingerprinting. *PLOS ONE* **8**, e73441 (2013).

18. N. V. Honch, J. S. O. McCullagh, R. E. M. Hedges, Variation of bone collagen amino acid $\delta^{13}\text{C}$ values in archaeological humans and fauna with different dietary regimes: Developing frameworks of dietary discrimination. *Am. J. Phys. Anthropol.* **148**, 495–511 (2012).
19. E. C. Webb, N. V. Honch, P. J. H. Dunn, G. Eriksson, K. Lidén, R. P. Evershed, Compound-specific amino acid isotopic proxies for detecting freshwater resource consumption. *J. Archaeol. Sci.* **63**, 104–114 (2015).
20. S. J. Garvie-Lok, T. L. Varney, M. A. Katzenberg, Preparation of bone carbonate for stable isotope analysis: The effects of treatment time and acid concentration. *J. Archaeol. Sci.* **31**, 763–776 (2004).
21. M. M. Beasley, E. J. Bartelink, L. Taylor, R. M. Miller, Comparison of transmission FTIR, ATR, and DRIFT spectra: Implications for assessment of bone bioapatite diagenesis. *J. Archaeol. Sci.* **46**, 16–22 (2014).
22. A. W. Froehle, C. M. Kellner, M. J. Schoeninger, FOCUS: Effect of diet and protein source on carbon stable isotope ratios in collagen: Follow up to Warinner and Tuross (2009). *J. Archaeol. Sci.* **37**, 2662–2670 (2010).
23. M. J. Wooller, G. D. Zazula, M. Edwards, D. G. Froese, R. D. Boone, C. Parker, B. Bennett, Stable carbon isotope compositions of eastern Beringian grasses and sedges: Investigating their potential as paleoenvironmental indicators. *Arct., Antarc., Alp. Res.* **39**, 318–331 (2007).
24. R. Fernandes, M.-J. Nadeau, P. M. Grootes, Macronutrient-based model for dietary carbon routing in bone collagen and bioapatite. *Archaeol. Anthropol. Sci.* **4**, 291–301 (2012).
25. L. Cordain, J. B. Miller, S. B. Eaton, N. Mann, S. H. Holt, J. D. Speth, Plant-animal subsistence ratios and macronutrient energy estimations in worldwide hunter-gatherer diets. *Am. J. Clin. Nutr.* **71**, 682–692 (2000).
26. M. Balasse, Reconstructing dietary and environmental history from enamel isotopic analysis: Time resolution of intra-tooth sequential sampling. *Int. J. Osteoarchaeol.* **12**, 155–165 (2002).

27. P. Mahoney, Incremental enamel development in modern human deciduous anterior teeth. *Am. J. Phys. Anthropol.* **147**, 637–651 (2012).
28. T. A. Cappiello, J. F. Bromaghin, Mark-recapture abundance estimate of fall-run chum salmon in the Upper Tanana River, Alaska, 1995. *Alaska Fishery Research Bulletin* **4**, 12–35 (1997).
29. B. A. Potter, A first approximation of Holocene inter-assemblage variability in central Alaska. *Arct. Anthropol.* **45**, 89–113 (2008).
30. B. A. Potter, C. E. Holmes, D. R. Yesner, Technology and economy among the earliest prehistoric foragers in interior eastern Beringia, in *Paleoamerican Odyssey*, K. E. Graf, C. V. Ketron, M. R. Waters, Eds. (Center for the Study of the First Americans, Texas A&M University, 2013), pp. 81–103.
31. K. Choy, B. A. Potter, H. J. McKinney, J. D. Reuther, S. W. Wang, M. J. Wooller, Chemical profiling of ancient hearths reveals recurrent salmon use in Ice Age Beringia. *Proc. Natl. Acad. Sci. U.S.A.* **113**, 9757–9762 (2016).
32. B. A. Potter, Models of faunal processing and economy in early Holocene interior Alaska. *Environ. Archaeol.* **12**, 3–23 (2007).
33. D. R. Yesner, Human dispersal into interior Alaska: Antecedent conditions, mode of colonization, and adaptation. *Quat. Sci. Rev.* **20**, 315–327 (2001).
34. C. M. Halfman, B. A. Potter, H. J. McKinney, B. P. Finney, A. T. Rodrigues, D. Y. Yang, B. M. Kemp, Early human use of anadromous salmon in North America at 11,500 y ago. *Proc. Natl. Acad. Sci. U.S.A.* **112**, 12344–12348 (2015).
35. B. A. Potter, E. P. Gaines, P. M. Bowers, M. Proue, “Results of the 2006 cultural resource survey of proposed Alaska Railroad northern rail extension routes and ancillary facilities, Alaska” (NLUR technical report #278b-c, Northern Land Use Research Inc., 2007).
36. H. T. Allen, *Report of an Expedition to the Copper, Tananá, and Kóyukuk Rivers, in the Territory of Alaska, in the Year 1885* (Government Printing Office, 1887).

37. C. Ballew, A. Ross, R. S. Wells, V. Hiratsuka, *Final Report on the Alaska Traditional Diet Survey* (Alaska Native Health Board, 2004).
38. S. J. AlQahtani, M. P. Hector, H. M. Liversidge, Accuracy of dental age estimation charts: Schour and Massler, Ubelaker and the London Atlas. *Am. J. Phys. Anthropol.* **154**, 70–78 (2014).
39. W. J. Pestle, B. E. Crowley, M. T. Weirauch, Quantifying inter-laboratory variability in stable isotope analysis of ancient skeletal remains. *PLOS ONE* **9**, e102844 (2014).
40. J. L. Barta, C. Monroe, B. M. Kemp, Further evaluation of the efficacy of contamination removal from bone surfaces. *Forensic Sci. Int.* **231**, 340–348 (2013).
41. B. M. Kemp, C. Monroe, K. G. Judd, E. Reams, C. Grier, Evaluation of methods that subdue the effects of polymerase chain reaction inhibitors in the study of ancient and degraded DNA. *J. Archaeol. Sci.* **42**, 373–380 (2014).
42. B. M. Kemp, K. Judd, C. Monroe, J. W. Eerkens, L. Hilldorfer, C. Cordray, R. Schad, E. Reams, S. G. Ortman, T. A. Kohler, Prehistoric mitochondrial DNA of domesticate animals supports a 13th century exodus from the northern US southwest. *PLOS ONE* **12**, e0178882 (2017).
43. B. M. Johnson, B. M. Kemp, Rescue PCR: Reagent-rich PCR recipe improves amplification of degraded DNA extracts. *J. Archaeol. Sci. Rep.* **11**, 683–694 (2017).
44. E. Palmer, S. Tushingham, B. M. Kemp, Human use of small forage fish: Improved ancient DNA species identification techniques reveal long term record of sustainable mass harvesting of smelt fishery in the northeast Pacific Rim. *J. Archaeol. Sci.* **99**, 143–152 (2018).
45. L. G. Jordan, C. A. Steele, G. H. Thorgaard, Universal mtDNA primers for species identification of degraded bony fish samples. *Mol. Ecol. Resour.* **10**, 225–228 (2010).
46. M. Buckley, V. L. Harvey, A. T. Chamberlain, Species identification and decay assessment of Late Pleistocene fragmentary vertebrate remains from Pin Hole Cave (Creswell Crags, UK) using collagen fingerprinting. *Boreas* **46**, 402–411 (2017).

47. T. B. Coplen, Guidelines and recommended terms for expression of stable-isotope-ratio and gas-ratio measurement results. *Rapid Commun. Mass Spectrom.* **25**, 2538–2560 (2011).
48. R. Longin, New method of collagen extraction for radiocarbon dating. *Nature* **230**, 241–242 (1971).
49. P. Szpak, J. Z. Metcalfe, R. A. Macdonald, Best practices for calibrating and reporting stable isotope measurements in archaeology. *J. Archaeol. Sci. Rep.* **13**, 609–616 (2017).
50. G. J. van Klinken, Bone collagen quality indicators for palaeodietary and radiocarbon measurements. *J. Archaeol. Sci.* **26**, 687–695 (1999).
51. S. H. Ambrose, Preparation and characterization of bone and tooth collagen for isotopic analysis. *J. Archaeol. Sci.* **17**, 431–451 (1990).
52. M. J. DeNiro, Postmortem preservation and alteration of in vivo bone collagen isotope ratios in relation to palaeodietary reconstruction. *Nature* **317**, 806–809 (1985).
53. M. P. Richards, P. B. Pettitt, E. Trinkaus, F. H. Smith, M. Paunović, I. Karavanić, Neanderthal diet at Vindija and Neanderthal predation: The evidence from stable isotopes. *Proc. Natl. Acad. Sci. U.S.A.* **97**, 7663–7666 (2000).
54. D. R. Guthrie, New carbon dates link climatic change with human colonization and Pleistocene extinctions. *Nature* **441**, 207–209 (2006).
55. B. A. Potter, J. D. Reuther, B. A. Newbold, D. T. Yoder, High resolution radiocarbon dating at the Gerstle River Site, central Alaska. *Am. Antiq.* **77**, 71–98 (2012).
56. F. B. Lanoë, J. D. Reuther, C. E. Holmes, G. W. L. Hodgins, Human paleoecological integration in subarctic eastern Beringia. *Quat. Sci. Rev.* **175**, 85–96 (2017).
57. J. A. Leonard, C. Vila, K. Fox-Dobbs, P. L. Koch, R. K. Wayne, B. Van Valkenburgh, Megafaunal extinctions and the disappearance of a specialized wolf ecomorph. *Curr. Biol.* **17**, 1146–1150 (2007).

58. P. Szpak, T. J. Orchard, D. R. Gröcke, A Late Holocene vertebrate food web from southern Haida Gwaii (Queen Charlotte Islands, British Columbia). *J. Archaeol. Sci.* **36**, 2734–2741 (2009).
59. S. P. Johnson, D. E. Schindler, Trophic ecology of Pacific salmon (*Oncorhynchus* spp.) in the ocean: A synthesis of stable isotope research. *Ecol. Res.* **24**, 855–863 (2009).
60. N. Misarti, B. Finney, H. Maschner, M. J. Wooller, Changes in northeast Pacific marine ecosystems over the last 4500 years: Evidence from stable isotope analysis of bone collagen from archeological middens. *The Holocene* **19**, 1139–1151 (2009).
61. K. Britton, E. McManus-Fry, O. Nehlich, M. Richards, P. M. Ledger, R. Knecht, Stable carbon, nitrogen and sulphur isotope analysis of permafrost preserved human hair from rescue excavations (2009, 2010) at the precontact site of Nunalleq, Alaska. *J. Archaeol. Sci. Rep.* **17**, 950–963 (2018).
62. D. A. Byers, D. R. Yesner, J. M. Broughton, J. B. Coltrain, Stable isotope chemistry, population histories and late prehistoric subsistence change in the Aleutian Islands. *J. Archaeol. Sci.* **38**, 183–196 (2011).
63. L. T. Corr, R. Berstan, R. P. Evershed, Optimisation of derivatisation procedures for the determination of $\delta^{13}\text{C}$ values of amino acids by gas chromatography/combustion/isotope ratio mass spectrometry. *Rapid Commun. Mass Spectrom.* **21**, 3759–3771 (2007).
64. R Core Team, R: A language and environment for statistical computing (R Foundation for Statistical Computing, 2017); www.R-project.org/.
65. C. J. Brown, M. T. Brett, M. F. Adame, B. Stewart-Koster, S. E. Bunn, Quantifying learning in biotracer studies. *Oecologia* **187**, 597–608 (2018).
66. H. Bocherens, D. G. Drucker, M. Germonpré, M. Lázničková-Galetová, Y. I. Naito, C. Wissing, J. Brůžek, M. Oliva, Reconstruction of the Gravettian food-web at Předmostí I using multi-isotopic tracking (^{13}C , ^{15}N , ^{34}S) of bone collagen. *Quat. Int.* **359-360**, 211–228 (2015).

67. M. L. Fogel, N. Tuross, D. W. Owsley, Nitrogen isotope tracers of human lactation in modern and archaeological populations, in *Annual report of the Director of the Geophysical Laboratory, 1988–1989* (Carnegie Institution, 1989), pp. 111–117.
68. A. de Luca, N. Boisseau, I. Tea, I. Louvet, R. J. Robins, A. Forhan, M. A. Charles, R. Hankard, $\delta^{15}\text{N}$ and $\delta^{13}\text{C}$ in hair from newborn infants and their mothers: A cohort study. *Pediatr. Res.* **71**, 598–604 (2012).
69. T. C. O'Connell, C. J. Kneale, N. Tasevska, G. G. C. Kuhnle, The diet-body offset in human nitrogen isotopic values: A controlled dietary study. *Am. J. Phys. Anthropol.* **149**, 426–434 (2012).
70. M. A. Vanderklift, S. Ponsard, Sources of variation in consumer-diet $\delta^{15}\text{N}$ enrichment: A meta-analysis. *Oecologia* **136**, 169–182 (2003).
71. B. C. Stock, B. X. Semmens, MixSIAR GUI user manual v3.1 (2016);
<https://github.com/brianstock/MixSIAR/>.
72. K. Choy, C. I. Smith, B. T. Fuller, M. P. Richards, Investigation of amino acid $\delta^{13}\text{C}$ signatures in bone collagen to reconstruct human palaeodiets using liquid chromatography–isotope ratio mass spectrometry. *Geochim. Cosmochim. Acta* **74**, 6093–6111 (2010).
73. M. Raghavan, J. S. O. McCullagh, N. Lynnerup, R. E. M. Hedges, Amino acid $\delta^{13}\text{C}$ analysis of hair proteins and bone collagen using liquid chromatography/isotope ratio mass spectrometry: Paleodietary implications from intra-individual comparisons. *Rapid Commun. Mass Spectrom.* **24**, 541–548 (2010).
74. E. C. Webb, N. V. Honch, P. J. H. Dunn, A. Linderholm, G. Eriksson, K. Lidén, R. P. Evershed, Compound-specific amino acid isotopic proxies for distinguishing between terrestrial and aquatic resource consumption. *Archaeol. Anthropol. Sci.* **10**, 1–18 (2018).
75. K. A. Hobson, R. G. Clark, Assessing avian diets using stable isotopes I: Turnover of ^{13}C in tissues. *The Condor* **94**, 181–188 (1992).

76. K. A. Hobson, L. Atwell, L. I. Wassenaar, T. Yerkes, Estimating endogenous nutrient allocations to reproduction in Redhead Ducks: A dual isotope approach using δD and $\delta^{13}\text{C}$ measurements of female and egg tissues. *Funct. Ecol.* **18**, 737–745 (2004).
77. D. R. Yesner, Faunal extinction, hunter-gatherer foraging strategies, and subsistence diversity among eastern Beringian Paleoindians, in *Foragers of the Terminal Pleistocene in North America*, R. B. Walker, B. N. Driskell, Eds. (University of Nebraska Press, 2007), pp. 15–31.
78. D. R. Yesner, Moose hunters of the boreal forest? A re-examination of subsistence patterns in the western subarctic. *Arctic* **42**, 97–108 (1989).
79. F. B. Lanoë, J. D. Reuther, C. E. Holmes, B. A. Potter, Small mammals and paleoenvironmental context of the terminal pleistocene and early holocene human occupation of central Alaska. *Geoarchaeology* **35**, 164–176 (2019).
80. R. A. McKennan, *The Upper Tanana Indians. Yale University Publications in Anthropology, No. 55* (Yale University, 1959).
81. M. P. Richards, R. E. M. Hedges, Variations in bone collagen $\delta^{13}\text{C}$ and $\delta^{15}\text{N}$ values of fauna from Northwest Europe over the last 40 000 years. *Palaeogeogr. Palaeoclimatol. Palaeoecol.* **193**, 261–267 (2003).
82. R. E. M. Hedges, R. E. Stevens, M. P. Richards, Bone as a stable isotope archive for local climatic information. *Quat. Sci. Rev.* **23**, 959–965 (2004).
83. D. H. Mann, P. Groves, M. L. Kunz, R. E. Reanier, B. V. Gaglioti, Ice-age megafauna in Arctic Alaska: Extinction, invasion, survival. *Quat. Sci. Rev.* **70**, 91–108 (2013).
84. B. Espinasse, B. P. V. Hunt, Y. D. Coll, E. A. Pakhomov, Investigating high seas foraging conditions for salmon in the North Pacific: Insights from a 100-year scale archive for Rivers Inlet sockeye salmon. *Can. J. Fish. Aquat. Sci.* **76**, 918–927 (2018).
85. E. Guiry, T. C. A. Royle, R. G. Matson, H. Ward, T. Weir, N. Waber, T. J. Brown, B. P. V. Hunt, M. H. H. Price, B. P. Finney, M. Kaeriyama, Y. Qin, D. Y. Yang, P. Szpak, Differentiating salmonid

- migratory ecotypes through stable isotope analysis of collagen: Archaeological and ecological applications. *PLOS ONE* **15**, e0232180 (2020).
86. B. A. Potter, J. D. Irish, J. D. Reuther, C. Gelvin-Reymiller, V. T. Holliday, A terminal Pleistocene child cremation and residential structure from eastern Beringia. *Science* **331**, 1058–1062 (2011).
87. C. R. Holloway, Paleoethnobotany in interior Alaska, thesis, University of Alaska Fairbanks (2016).
88. M. J. Sheriff, R. Boonstra, R. Palme, C. L. Buck, B. M. Barnes, Coping with differences in snow cover: The impact on the condition, physiology and fitness of an arctic hibernator. *Conserv. Physiol.* **5**, cox065 (2017).
89. C. L. Buck, B. M. Barnes, Annual cycle of body composition and hibernation in free-living arctic ground squirrels. *J. Mammal.* **80**, 430–442 (1999).
90. M. J. Sheriff, C. L. Buck, B. M. Barnes, Autumn conditions as a driver of spring phenology in a free-living arctic mammal. *Clim. Change Resp.* **2**, 4, (2015).
91. L. Halpin, *Living Off the Land: Contemporary Subsistence in Tetlin, Alaska* (Alaska Department of Fish and Game, 1987).
92. M. Trotter, B. B. Hixon, Sequential changes in weight, density, and percentage ash weight of human skeletons from an early fetal period through old age. *Anat. Rec.* **179**, 1–18 (1974).
93. A. Rohatgi, WebPlotDigitizer Version 4.1 (2018); <https://automeris.io/WebPlotDigitizer>.
94. K. Nakano, T. Iwamatsu, C. M. Wang, M. Tarasima, T. Nakayama, K. Sasaki, E. Tachikawa, N. Noda, E. Mizoguchi, M. Osawa, High bone turnover of type I collagen depends on fetal growth. *Bone* **38**, 249–256 (2006).
95. R. W. Leggett, K. F. Eckerman, L. R. Williams, Strontium-90 in bone: A case study in age-dependent dosimetric modeling. *Health Phys.* **43**, 307–322 (1982).
96. F. Rauch, E. Schoenau, Changes in bone density during childhood and adolescence: An approach based on bone's biological organization. *J. Bone Miner. Res.* **16**, 597–604 (2001).

97. J. W. Wood, *Dynamics of Human Reproduction: Biology, Biometry, Demography* (Aldine De Gruyter, 1994).
98. P. M. Bowers, J. D. Reuther, AMS re-dating of the Carlo Creek Site, Nenana Valley, central Alaska. *Curr. Res. Pleist.* **25**, 58–61 (2008).
99. B. A. Potter, J. D. Reuther, Site chronology, in *Archaeological Investigations at Delta River Overlook*, B. A. Potter, Ed. (Archaeology GIS Laboratory, University of Alaska Fairbanks, 2018), pp. 58–70.
100. B. A. Potter, Radiocarbon chronology of central Alaska: Technological continuity and economic change. *Radiocarbon* **50**, 181–204 (2008).
101. M. J. Wooller, J. Kurek, B. V. Gaglioti, L. C. Cwynar, N. Bigelow, J. D. Reuther, C. Gelvin-Reymiller, J. P. Smol, An ~11,200 year paleolimnological perspective for emerging archaeological findings at Quartz Lake, Alaska. *J. Paleolimnol.* **48**, 83–99 (2012).
102. B. A. Potter, Site structure and organization in Central Alaska: Archaeological investigations at Gerstle River, thesis, University of Alaska Fairbanks (2005).
103. B. Shapiro, A. J. Drummond, A. Rambaut, M. C. Wilson, P. E. Matheus, A. V. Sher, O. G. Pybus, M. T. P. Gilbert, I. Barnes, J. Binladen, E. Willerslev, A. J. Hansen, G. F. Baryshnikov, J. A. Burns, S. Davydov, J. C. Driver, D. G. Froese, C. R. Harrington, G. Keddie, P. Kosintsev, M. L. Kunz, L. D. Martin, R. O. Stephenson, J. Storer, R. Tedford, S. Zimov, A. Cooper, Rise and fall of the Beringian steppe bison. *Science* **306**, 1561–1565 (2004).
104. M. Meiri, A. M. Lister, M. J. Collins, N. Tuross, T. Goebel, S. Blockley, G. D. Zazula, N. van Doorn, R. Dale Guthrie, G. G. Boeskorov, G. F. Baryshnikov, A. Sher, I. Barnes, Faunal record identifies Bering isthmus conditions as constraint to end-Pleistocene migration to the New World. *Proc. Biol. Sci.* **281**, 20132167 (2014).
105. J. P. Cook, Historic archaeology and ethnohistory at Healy Lake, Alaska. *Arctic* **42**, 109–118 (1989).

106. S. E. Alter, S. D. Newsome, S. R. Palumbi, Pre-whaling genetic diversity and population ecology in eastern Pacific gray whales: Insights from ancient DNA and stable isotopes. *PLOS ONE* **7**, e35039 (2012).
107. C. R. Harington, Ed., *Annotated Bibliography of Quaternary Vertebrates of Northern North America* (University of Toronto Press, 2003).
108. R. G. Harrison, M. A. Katzenberg, Paleodiet studies using stable carbon isotopes from bone apatite and collagen: Examples from Southern Ontario and San Nicolas Island, California. *J. Anthropol. Archaeol.* **22**, 227–244 (2003).
109. E. J. Bartelink, Resource intensification in pre-contact central California: A bioarchaeological perspective on diet and health patterns among hunter-gatherers from the lower Sacramento Valley and San Francisco Bay, thesis, Texas A&M University (2006).
110. J. Tackney, J. Coltrain, J. Raff, D. O'Rourke, Ancient DNA and stable isotopes: Windows on Arctic prehistory, in *The Oxford Handbook of the Prehistoric Arctic*, T. M. Friesen, O. K. Mason, Eds. (Oxford Univ. Press, 2016), pp. 51–79.